March 2017

An Adult Zebrafish Brain Atlas To Investigate Shh Mediated Cell-Cell Signaling In Neurogenic Zones

Alyssa P. Lutservitz
University of Massachusetts Amherst

AN ADULT ZEBRAFISH BRAIN ATLAS TO INVESTIGATE SHH MEDIATED CELL-CELL SIGNALING IN NEUROGENIC ZONES

A Thesis Presented

by

ALYSSA LUTSERVITZ

Submitted to the Graduate School of the

University of Massachusetts Amherst in partial fulfillment

of the requirements for the degree of

MASTER OF SCIENCE

February 2017

Neuroscience and Behavior

AN ADULT ZEBRAFISH BRAIN ATLAS TO INVESTIGATE SHH MEDIATED CELL-CELL SIGNALING IN NEUROGENIC ZONES

A Thesis Presented

by

ALYSSA LUTSERVITZ

Approved as to style and content by:

Rolf Karlstrom, Chair

Joseph Bergan, Member

Alicia Timme-Laragy, Member

Gerald Downes, Member

Betsy Dumont, Department Head
Neuroscience and Behavior

ACKNOWLEDGEMENTS

I would like to thank my committee chair and advisor, Dr. Rolf Karlstrom, for providing helpful insight and guidance. It has been a great opportunity to work in his lab over the past few years. A huge thanks to the members of the Karlstrom lab for their support during this time.

I would also like to thank my committee members for offering helpful feedback and advice. Thank you Dr. Joseph Bergan, Dr. Alicia Timme-Laragy, and Dr. Gerald Downes. Your guidance has been greatly appreciated.

A final thanks to the friends and family that have and continue to support me in all of my endeavors – academic and beyond.

ABSTRACT

AN ADULT ZEBRAFISH BRAIN ATLAS TO INVESTIGATE SHH MEDIATED CELL-CELL SIGNALING IN NEUROGENIC ZONES

FEBRUARY 2017

ALYSSA LUTSERVITZ, B.S., UNIVERSITY OF MASSACHUSETTS AMHERST

M.S., UNIVERSITY OF MASSACHUSETTS AMHERST

Directed by: Dr. Rolf Karlstrom

Adult neurogenesis occurs in proliferative zones of the brain that contain neural progenitor cell populations capable of differentiating into specific cell types. However, we remain limited in our understanding of the signals that regulate neural progenitor cell proliferation and differentiation in adults. Recently zebrafish (*Danio rerio*) have emerged as an excellent model for studying the molecular mechanisms behind adult neurogenesis, because sixteen proliferative zones remain active in the adult brains. Thousands of fluorescent transgenic reporter lines have been generated in zebrafish that reveal gene expression patterns of cell-cell signaling systems, some of which may regulate neurogenesis in these brain regions. Using a new tissue clearing technique and whole brain imaging with fluorescent light sheet microscopy (FLSM) we have generated the first 3-Dimensional atlas of gene expression in an intact adult zebrafish brain. So far we have created a reference brain image and have aligned the expression patterns from three transgenic lines. This work is a preliminary step in the generation of a new, open access brain atlas called the Zebrafish Adult Brain Browser (ZABB). While generating this atlas we focused on documenting the adult brain regions responsive to Sonic Hedgehog (Shh), a cell-cell signaling system known to regulate neurogenesis during embryonic development. We used two Shh-reporter lines to create another atlas comparing reporter transgene expression in whole brain and sectioned tissue to the expression of the Hedgehog (Hh) target gene *ptch2* using

in situ hybridization. We show that the reporter lines reveal different Hh responsive domains, but together identify fourteen Hh responsive regions in the brain, nine of which are known proliferative zones. Thus, it appears that subsets of both proliferating neural progenitors and non-proliferative cells remain Hh responsive in adult brains. Our data suggests that Hh signaling contributes to the regulation of neural progenitor cells in nine of the sixteen proliferative zones. Uncovering the molecular mechanisms behind adult neurogenesis and forming a greater understanding of adult neural stem cell regulation has the potential to influence the treatment of many neurodegenerative diseases and cancers.

TABLE OF CONTENTS

Page

LIST OF TABLES

LIST OF FIGURES

CHAPTER 1

ZEBRAFISH AS A MODEL TO UNDERSTAND ADULT NEUROGENESIS

The brain consists of billions of neuronal and glial cells that function in complex neural networks to direct processes and behaviors essential for sustaining life. In order to form an understanding of this complex organ we have generated brain atlases. These atlases act as road maps by allowing researchers to navigate through the nervous system. There are currently brain atlases for several model systems that provide detailed information on anatomy, gene expression, and connectivity, while forming a foundation for functional analyses (Jones et al., 2009; Milyaev et al., 2012; Ronneberger et al., 2012). Atlases have been essential for the careful and thoughtful planning of experiments geared toward the function of neural circuits and the discovery of complex neural networks underlying behavior, which have helped to begin unravel the complex relationship between brain structure and function (Randlett et al., 2015). For my Master's thesis I have helped generate two adult zebrafish brain atlases: a 3-Dimensional gene expression atlas using whole brain imaging with fluorescent light sheet microscopy (FLSM) and an atlas of Sonic hedgehog (Shh) signaling in adult neurogenic regions of the brain. My hope is to convey the usefulness and various applications for brain atlases in neuroscience research.

While several larval zebrafish brain atlases exist, the only available brain atlas for the adult zebrafish is based on sectioned tissue and lacks information on gene expression and connectivity (Wullimann et al., 1996; Arrenberg and Driever, 2013). To account for the lack of an adult expression atlas, as well as the growing interest in adult brain function using zebrafish as a model, we have created the Zebrafish Adult Brain Browser (ZABB), a 3-Dimensional gene expression atlas of the adult zebrafish brain created with whole brain imaging using FLSM. In Chapter 2 I discuss a new tissue clearing technique similar to CLARITY used to generate

transparent intact adult brains capable of whole mount imaging (Tomer et al., 2014; Menegas et al., 2015). So far we have optimized tissue and image processing pipelines, generated the first adult reference brain image, mapped gene expression data from three transgenic lines onto the atlas, and begun anatomical annotation of brain regions. High resolution imaging with FLSM has enabled us to identify the location of specific cell types and observe cellular morphology and projections within a whole brain, eliminating the need for tissue sectioning. Antibody labeling of whole adult brains is being developed as a new technique that will vastly increase the number of cellular and molecular features that can be added to the atlas. With this atlas, we can perform post-hoc analysis of neural activity and map neural connections in an adult brain for the first time, providing the neuroscience community with new tools that other atlases currently lack.

In Chapter 3 I discuss the creation of an atlas documenting Shh mediated cell-cell signaling in adult zebrafish brain proliferative zones. The Hedgehog (Hh) signaling pathway is one of several highly conserved cell-cell signaling systems known to regulate the proliferation of neural stem cell populations in both mammalian and zebrafish brains (reviewed in Briscoe and Therond, 2013; Alvarez-Buylla, 2014). To form a better understanding of where Hh signaling functions in adult zebrafish brains, we created an atlas of Hh responsive cells in the adult brain by examining the expression of the Hh target gene *ptch2* (by *in situ* hybridization) and by documenting expression of fluorescent proteins driven in transgenic fish by a ~1.2kb *ptch2* DNA regulatory element. We compared fluorescent protein expression in six different Hh-reporter lines and found that transgene expression in nuclear-tagged GFP and mCherry most faithfully recapitulated *ptch2* mRNA expression. Using both tissue sections and whole brain imaging with FLSM we identified fourteen Hh responsive regions in the adult brain. We found that nine of the sixteen identified proliferative zones in the adult zebrafish brain contain Hh responsive cells,

seven of which are in ventricular regions (Grandel et al., 2006). The two non-ventricular Hh responsive proliferative zones are located at the border between the olfactory bulbs (OBs) and dorsal telencephalon (D) and in the torus longitudinalis (TL). The remaining five Hh responsive regions: the olfactory bulbs (OBs), dorsal entopenduncular nucleus (End), preglomerular nucleus (PGm), and distinct cells in the midbrain and hindbrain, have not been identified as proliferative zones in adult zebrafish. Thus, it appears that subsets of both proliferating neural progenitors and non-proliferative cells remain responsive to Hh in the adult.

We hope this work will contribute to a better understanding of the factors regulating neural stem cell proliferation and differentiation in the adult vertebrate brain, knowledge that will be key to the development of stem cell therapies to treat neurodegenerative diseases and cancers. By adding expression data from the Hh reporter lines to the ZABB we have the ability to visualize the connections between Hh responsive cells in proliferative zones and to form a better understanding of the role of Hh in adult neurogenesis. With the addition of gene expression data from a variety of transgenic lines to the ZABB, we will be able to identify other cell-cell signaling systems and cell types that may play an important role in adult neurogenesis. With an increased interest in adult brain function using zebrafish as a model, the ZABB will be useful in many areas of adult brain research not restricted to neurogenesis. This atlas may also serve as an important tool for the careful planning and evaluation of experiments designed to understand regeneration, neural circuitry, simple and complex behaviors, aging, and disease.

CHAPTER 2

ZEBRAFISH ADULT BRAIN BROWSER (ZABB): A 3-DIMENSIONAL ANNOTATED ATLAS OF GENE EXPRESSION IN ADULT ZEBRAFISH BRAINS USING WHOLE BRAIN IMAGING WITH FLUORESECNT LIGHT SHEET MICROSCOPY (FLSM)

A. Introduction

Since the time of Camillo Golgi and Ramòn y Cajal, the ability to visualize and map neural connections in the brain has transformed neuroscience research (reviewed in Grant, 2006; De Carlos and Borrell, 2007; Wilt et al., 2010). With improvements in microscopy and tissue preparation, brain atlases have been developed that allow scientists to navigate through a scaffold of the nervous system. The first complete mapping of the nervous system was accomplished in the nematode *(Caenorhabditis elegans)* (White et al., 1986). Both the structure and connectivity of the nervous system were mapped using electron micrograph serial sections. While this was a landmark achievement, the complete nematode nervous system consists of only 302 total neurons, which is relatively simple in comparison to complex nervous systems, such as adult humans who have an average of 86 billion neurons (White et al., 1986; Herculano-Houzel, 2012). However, the connectome has been important in the planning of experiments that have helped scientists understand simple circuits and complex neural networks underlying behavior.

There are currently brain atlases for several organisms, including mouse, fly, embryonic and larval zebrafish, non-human primate, and human (Jones et al., 2009; Milyaev et al., 2012; Ronneberger et al., 2012; Marquart et al., 2015; Randlett et al., 2015). The most well-known brain atlas is the Allen Brain Atlas, which is an important resource to many neuroscientists. The Allen Institute has developed atlases for the adult and developing mouse, non-human primate, and human brains (reviewed in Jones et al., 2009; Sunkin et al., 2013). These atlases provide

many resources, including detailed gene expression data, connectivity and projection mapping, anatomical and histological information, *in situ* hybridization (ISH), and magnetic resonance imaging (MRI) data. All resources have been made available to the public in an easily navigated and interactive online data portal that serves not only the entire neuroscience community, but policy makers and the general public as well.

The Virtual Fly Brain is an impressive example of a community based 3-Dimensional adult brain atlas that includes gene expression, connectivity, and neuroanatomical information (Milyaev et al., 2012). This atlas uses an open-source model that allows researchers to easily add expression data and has become a catalyst for collaborative research within the fly community. Several 3-Dimensional zebrafish brain atlases have recently been developed that take advantage of the optical clarity of embryonic and larval fish. These atlases have begun to catalogue the expression of transgenic fluorescent reporter lines onto a reference brain image (Ronneberger et al., 2012; Marquart et al., 2015; Randlett et al., 2015; reviewed in Arrenberg and Driever, 2013). However, due to the lack of optical clarity in adult zebrafish, the only available atlas for the adult brain is based on histological sections (Wullimann et al., 1996).

Historically, zebrafish have been a powerful model for investigating the molecular mechanisms that guide embryonic brain development. Recently, there has been increased interest in studying post-embryonic and adult brain activity using zebrafish as a model, due to the conserved structure of the vertebrate brain and their experimental tractability. Live functional brain imaging and phosphorylated ERK (pERK) labeling of neuronal activity in larval zebrafish has led to an understanding of whole-brain activity patterns associated with many simple and complex behaviors (Randlett et al., 2015). In addition, the ability to monitor neural activity from larval stages to adulthood may provide a functional understanding of the brain throughout life

and enable us to potentially monitor disease and the process of aging. The adult zebrafish nervous system continues to grow throughout life and has remarkable regenerative abilities, making zebrafish an excellent model for studying the molecular mechanisms involved in neural stem cell (NSC) proliferation and differentiation in adult brains (Reimer et al., 2009; Grandel et al., 2006).

To facilitate the increased research effort on adult brain function, we have developed a 3-Dimensional, gene expression atlas of the adult zebrafish brain that will eventually be made available to the scientific community as an online, open-source atlas called the Zebrafish Adult Brain Browser (ZABB). We have optimized a tissue clearing technique similar to CLARITY (Chung and Deisseroth, 2013; Tomer et al., 2014) that allows us to produce transparent, intact adult brains that can be imaged quickly and at high resolution using fluorescent light sheet microscopy (FLSM). This technique allows us to image gene expression patterns from fluorescent transgenic lines, as well as antibody labeling, in whole brains. A reference brain has been generated that allows us to register new expression data and potentially compare the expression of thousands of transgenic lines and antibody markers that are available to the zebrafish community. This technique will provide insight on the complex cytoarchitecture of the adult vertebrate brain and enable us to form a better understanding of the relationship between structure, function, and dysfunction in the nervous system.

B. Methods

i. Brain dissection

Adult zebrafish from fifteen different transgenic lines, ranging from one month to three years of age, were selected for the atlas (Supplementary Table S2.1). Standard length and sex

were recorded prior to the dissection of each fish. Fish were first anesthetized in MS-222 and once movement ceased were transferred to a petri dish of cold (4°C) phosphate buffered saline (PBS). The head was quickly removed with a scalpel at a location just anterior to the pectoral fin. The head was then steadied in a dorsal orientation with a pair of forceps positioned at the opercula and the skull cap was removed, exposing the dorsal surface of the brain. Next, both eyes were removed by cutting through the optic nerve with a pair of scissors. The head was then positioned and steadied in a ventral orientation and lateral cuts were made along the jaw with scissors. Forceps were used to remove the jaw and the remaining tissue and bone surrounding the brain. The pituitary gland and occasionally the olfactory bulbs were removed during dissection. A method that prevents the removal of these structures may be necessary to provide a full description of the adult central nervous system. A dorsal and ventral view of a dissected adult brain can be seen in Supplemental Figure S2.1A.

ii. Hydrogel fixation and polymerization

Dissected brains were transferred to individually labeled Eppendorf tubes containing 1mL of cold (4°C) hydrogel (4% wt/vol acrylamide, 0.05% wt/vol bisacrylamide, 4% wt/vol PFA, 0.25% wt/vol VA-044 thermal initiator (Wako Chemicals); Tomer et al., 2014). The tubes were then covered with aluminum foil and fixed for 24 hours at 4°C. During fixation, paraformaldehyde (PFA) in the hydrogel solution served to both covalently bind acrylamide and bisacrylamide monomers to biomolecules in the tissue, such as proteins, nucleic acids, and other small molecules, and to crosslink these biomolecules to one another via amine groups (Tomer et al., 2014). Hydrogel was stored in small quantities in the dark at 20°C and kept on ice during use to prevent activation of the heat and light sensitive VA-044 thermal initiator (Wako Chemicals).

Leaving hydrogel at room temperature and consistently rethawing hydrogel caused unwanted polymerization to occur.

Fixed and dorsally-oriented brains were polymerized in fresh, degassed hydrogel overnight at 37°C in a plexiglass polymerization mold (Supplemental Figure S2.1B). Incubation at 37°C activated the VA-044 thermal initiator (Wako Chemicals), which initiated hydrogel polymerization and thereby preserved the structural framework of biomolecules within the brain. Degassing reduced the amount of oxygen dissolved in the hydrogel, which eliminated the appearance of bubbles in polymerized hydrogel. Bubbles still formed along the surface of the polymerized hydrogel in the mold (Supplemental Figure S2.1B), but disappeared once the mold was disassembled.

iii. Passive and active clearing of lipids

The polymerized sheet of hydrogel and brains was carefully removed from the mold with a metal spatula and placed in a petri dish of fresh SDS/borate clearing (SBC) buffer, a strong ionic detergent used to remove lipids from fixed and polymerized brains (4% wt/vol SDS in 0.2M boric acid buffer (pH = 8.5) final concentration/ 20% wt/vol SDS in 1M boric acid buffer (pH = 8.5) stock solution diluted five-fold in ddH2O; Tomer et al, 2014). The polymerized sheet was then cut into small rectangular blocks around the brains using a razor blade. Since PFA in the hydrogel solution does not cross link with lipids in the tissue, they were removed from the brains in either a passive or active clearing process (Tomer et al., 2014). For passive clearing, each block was transferred to an Eppendorf tube containing 1mL of fresh SBC buffer and kept at 37°C. A loss of fluorescence in transgenic brains has been attributed to the use of old SBC buffer during lipid-clearing. To account for this, SBC buffer was made close to the time brains would be cleared and was changed daily. The pH of the SBC buffer was also monitored, as a pH of 8.5

was necessary for effective passive clearing of the tissue. Active clearing used a current to move SBC buffer through the brain tissue and greatly accelerated the clearing process. Adequate passive clearing of an adult zebrafish brain took approximately five to seven days, while active clearing produced lipid-cleared brains in twelve hours. Sufficient lipid-clearing was necessary for optimal imaging with FLSM and antibody labeling of whole brains.

iv. Refractive index homogenization with Optiview

After passive or active lipid-clearing, polymerized blocks were washed in boric acid buffer (0.2M, pH 8.5, with 0.1% Triton X-100; Tomer et al., 2014) for 24 hours in the dark at room temperature. This washing step drives SDS from the SBC buffer out of the brain for optimal imaging with FLSM. Blocks were then transferred to clean Eppendorf tubes containing 1mL of Optiview (RI=1.45) (patent pending). Optiview renders the intact brain transparent in light within three hours at room temperature (Supplemental Figure S2.1C) and within an hour at 37°C. Imaging with FLSM was optimal when Optiview had a refractive index of 1.45 and when blocks were imaged in the same Optiview that was used for refractive index homogenization.

v. Fluorescent light sheet microscopy (FLSM)

A small magnet was superglued to the dorsal surface of a block. Since the polymerization mold had a height of 8mm, this left 4-5mm of hydrogel between the super glue affixed magnet and brain tissue, which decreased interference from the magnet during imaging. The magnet superglued to the block was then affixed to a magnet located on a glass capillary tube within a Light Sheet Microscope (Zeiss). The glass capillary and magnet mounted block were then manually lowered into the imaging chamber (n-1,45 5x) containing 20mL of Optiview (RI=1.45).

Entire adult zebrafish brains were imaged in the transverse plane from anterior to posterior using a 5x lens. Four different channels, representing different wavelengths of light (405, 488, 561, and 638nm), were used to image real fluorescent expression data and autofluorescence within the brain. Whole brain z-stack images obtained with FLSM were then resized to 5µm/pixel resolution in Image J for later processing. A whole brain transverse z-stack image at the anterior midbrain from the transgenic line *Tg(-2.7shha:GFP)* can be seen in Supplementary Figure S2.1D.

vi. Antibody labeling intact adult zebrafish brains

Following the washing step in boric acid buffer as described above, brains were placed in a 10x concentration of primary antibody in PBS with 0.01% sodium azide. Sodium azide prevented bacterial growth during incubations and increased the shelf life of the antibody solution. The tubes were covered with aluminum foil and incubated on a shaker at 37°C for 2 weeks. Brains were then removed from the primary antibody solution and washed in PTX (PBS with 0.1% triton-x) for 1-2 days at 37°C. Next, brains were placed in a 10x concentration of secondary antibody in PBS with 0.01% sodium azide. Tubes were again covered with aluminum foil, incubated on a shaker at 37°C for 2 weeks, and then washed in PTX for 1-2 days at 37°C. After the final wash, brains were placed in Optiview for refractive index homogenization prior to imaging with FLSM. Our current protocol for antibody labeling whole adult zebrafish brains has achieved 1mm of antibody penetration in approximately one month.

Primary and secondary antibodies used to test this protocol include: anti-mCh/RFP (Rabbit) 1:50 (MBL PM005), anti-acetylated tubulin (Mouse/IgG2b) 1:100 (Sigma), anti-PCNA (Mouse/IgG2a) 1:50 (Sigma p8825), goat-anti-rabbit IgG Alexa 546 1:80 (A11010), goat-anti-

mouse IgG2b Alexa 546 1:80 (Molecular Probes), and goat-anti-mouse IgG2a Alexa 488 1:80 (A21131). The primary and secondary antibody solutions were stored at 4°C for future use.

C. Results

i. Mapping expression data from zebrafish transgenic lines onto an adult reference brain

We have generated the first reference brain for the adult zebrafish (Figure 2.1) at 5µm/pixel resolution using Elastix software and Matlab scripts that previously generated a 5µm/pixel resolution reference brain for mouse (Menegas et al., 2015; Klein et al., 2010). The reference brain was created by aligning transverse z-stack images of an intact, transparent brain from a 30mm adult zebrafish imaged at 5x using FLSM. Autofluorescent channels were used to generate the reference brain image, which serves as a scaffold for mapping gene expression data.

We have collected images spanning the entire brain, from olfactory bulbs to hindbrain, of three fluorescent transgenic lines *Tg(tcfsiam:GFP), Tg(GBS:ptch2:nlsGFP),* and *Tg(GBS-ptch2:nlsmCh)*). We imaged entire brains with four wavelengths of light (405, 488, 561, and 638nm) to capture real gene expression data reported by the transgenic lines, as well as autofluorescence in the brain tissue and vasculature. The z-stack images from an autofluorescent channel of an imaged transgenic brain were selected for initial alignment to the reference brain. We then used Transformix software to align the remaining autofluorescent channels and the channel with real fluorescent expression data.

We have currently aligned the expression patterns from the three transgenic lines to the reference brain (Figure 2.1A). Since the reference brain is composed of aligned autofluorescent channels, we determined that bright areas in certain regions of the brain and within vasculature indicated overlap in these channels (Figure 2.1B). We believe that fluorescence in these regions

found in imaged transgenic brains does not represent real expression. An exception to this assumption is the Wnt-reporter line *Tg(Ttcfsiam:GFP)*, which displays bright fluorescent transgene expression in brain vasculature (Figure 2.1C). Upon closer examination, we found that individual cells within the blood vessels were expressing the transgene, which may indicate a role for Wnt in blood cells (data not shown). Autofluorescence was also found in vasculature in both nuclear Hh reporter lines, *Tg(GBS-ptch2:nlsGFP*) and *Tg(GBS-ptch2:nlsmCh)* (Figures 2.1D-E). Additionally, we found bright transgene expression from all three lines along the posterior recess (PR) of the diencephalic ventricle (DIV) (Figure 2.1A). In this region, Wnt-responsive cells and Hh-responsive cells are distinct. Wnt responsive cells are found along the dorsal region of the PR (Figure 2.1C), while Hh-responsive cells are found along the medial and ventral regions of the PR (Figures 2.1D-E). The nuclear-GFP line expresses its transgene in a larger subset of Hh-responsive cells in this region (Figure 2.1D), than the nuclear-mCherry line (Figure 2.1E), which may be due to differences in location of transgene insertion in the two lines.

ii. Color-coded anatomical annotation of the reference brain

We used standardized neuroanatomical terms and ontology codes curated on Zebrafish Information Network (ZFIN) to annotate adult brain regions. Using z-stack images of the reference brain in several different planes (Figure 2.2A), we manually outlined broad brain regions and assigned each a unique color value. Color-coded anatomical annotation of major brain regions was performed on the reference brain in the transverse (Figure 2.2B), sagittal (Figure 2.2C), and horizontal (Figure 2.2D) plane. After broad brain regions have been annotated, the work will be expanded to include more refined brain regions. The annotation of smaller and less histologically identifiable brain regions will be aided by the addition of

expression data from transgenic lines and antibody labeling of specific cell types known within those regions.

iii. Comparing reporter gene expression across fifteen transgenic lines

We selected fifteen GFP and mCherry expressing transgenic lines for the generation of the Zebrafish Adult Brain Browser (ZABB) (Supplemental Table S2.1). These lines have been used to study the embryonic roles of Shh-, Wnt-, FGF-, Retinoic Acid, Notch, and BMP-mediated cell-cell signaling, as well as lines that label neuronal and glial cell populations (see references in Supplemental Table S2.1). Ten of the fifteen transgenic lines show fluorescent protein expression in sectioned adult brain tissue (Supplemental Table S2.1). Out of the ten lines with known adult expression, whole brains from nine of the lines were imaged with FLSM, and all but one displayed expression patterns comparable to sectioned tissue using a 5x lens (Supplemental Table S2.1). In the remaining line, weak fluorescent protein expression in the brain was regained using a 20x lens (Supplemental Table S2.1).

We found that cleared brain tissue imaged with FLSM produced accurate expression patterns when compared to sectioned brain tissue (Supplemental Figure S2.2). However, fluorescence was generally not as bright as in sectioned tissue and fluorescence was only observed in ~10% of brains from known transgenic fish, which is likely due to inconsistencies in tissue preparation. The relative level of transgene expression, as well as sub-cellular targeting of fluorescent proteins, had a major impact on the utility of a line for imaging with FLSM. The expression of Shh producing cells in the line *Tg(-2.7shha:GFP)* was similar in both sectioned (Figure S2.2A) and transparent (Figure S2.2B) tissue. Areas of the brain with strong GFP expression were easily imaged, while areas with weak expression, such as the diencephalic ventricle (DIV) were not. Along the DIV, GFP expressing cells are found closely lining the

ventricle in sectioned tissue (Figure S2.2A). However, cleared tissue imaged with FLSM only shows a few GFP expressing cells restricted to one region (Figure S2.2B). This shows FLSM is best at capturing areas of high fluorescent protein expression using a 5x lens, but areas with weak expression levels are often missed. A 20x lens may be used to capture weak fluorescent protein expression displayed by transgenic lines. As an example, the cytoplasmic-GFP Hh reporter line, *Tg(GBS-ptch2:GFP),* displayed strong GFP expression in the ventral hypothalamus in sectioned tissue, but did not display any fluorescent expression when imaged at 5x with FLSM (data not shown; Supplemental Table S2.1). However, expression was observed at 20x magnification (Supplemental Table S2.1).

While both GFP and mCherry fluorescent proteins were imaged successfully with FLSM, the detection of mCherry was less sensitive compared to GFP detection. Comparing the nuclear-GFP and nuclear-mCherry fluorescent protein expressing Hh reporter lines, *Tg(GBS-ptch2:nlsGFP)* and *Tg(GBS-ptch2:nlsmCh),* revealed that GFP expressing cell nuclei imaged with FLSM are brighter and appear more similar to the expression pattern observed in sectioned tissue than mCherry expressing cell nuclei (Figures S2.2C-F). Even with the careful adjustment of laser power levels and detection parameters, mCherry still appears relatively weak when imaged with FLSM (Figure S2.2F), even though transgene expression in sectioned tissue is bright (Figure S2.2E).

In the nuclear-GFP line, *Tg(GBS-ptch2:nlsGFP),* GFP expressing cell nuclei are located along the lateral recess (LR) of the DIV (Figure S2.2C), in a pattern similar to the GFP expressing Shh producing cells lining the DIV in the line *Tg(-2.7shha:GFP)* (Figure S2.2A). However, since the nuclear-GFP line accumulates GFP in only the nuclei of expressing cells, the relative transgene expression is greater than in cells that express GFP in the cytoplasm, such as

the line *Tg(-2.7shha:GFP).* Therefore, based on the strong transgene expression, GFP expressing cell nuclei are comparable in both sectioned (Figure S2.2C) and transparent (Figure S2.2D) brain tissue along the LR of the DIV, unlike the expression observed along the DIV in both sectioned and transparent brain tissue from the line *Tg(-2.7shha:GFP)* (Figure S2.2A-B).

Therefore, we found that the relative level of transgene expression, the intensity of the fluorescent protein used, and the sub-cellular localization of fluorescent proteins affected imaging of whole brains with FLSM. Imaging was optimal in regions of the brain with high levels of transgene expression and in lines that utilized higher intensity fluorescent protein, such as GFP. We also found that transgenic lines that accumulated fluorescent proteins within the nucleus of expressing cells could be imaged with FLSM in regions where only a few cells were found, unlike transgenic line where GFP was distributed throughout the cytoplasm. Imaging lines with weak transgene expression and lines that utilize weaker fluorescent proteins, such as mCherry, may be enhanced with FLSM using a 20x lens.

iv. Distinguishing cellular morphology and type with FLSM

Imaging whole adult zebrafish brains with FLSM allowed visualization of cellular morphology and projections, as well as the location of distinct cell types. BMP responsive cellular projections from the transgenic line *Tg(bre:GFP*) are observed along the caudal lobe of the cerebellum using a 5x lens (Figure 2.3A). Both cellular morphology and projection location are seen in z-stack images through this region of the brain. Wnt (green) and Hh (red) responsive cells were observed in distinct regions of the posterior recess (PR) of the diencephalic ventricle at 20x in the double transgenic *Tg(GBS-ptch2:nlsmCh x tcfsiam:GFP*) (Figure 2.3B). Wnt and Hh responsive cells in this region indicate that both signaling proteins act on a subset of different cells in the PR. The information acquired with whole brain imaging using FLSM may provide

information on connections within the brain, as well as the type and morphology of cells residing in certain brain regions.

v. Antibody labeling whole adult zebrafish brains

We found that longer incubations times enabled deeper antibody penetration into the brain. We began with three day incubations of both primary and secondary antibody and saw that labeling was restricted to the surface of the brain tissue, which indicated that the antibodies were unable to penetrate into the tissue in this time period (data not shown). We then extended both primary and secondary antibody incubations to one week and saw improved results with antibody penetration up to 500µm into the brain. By extending the incubations of both primary and secondary antibodies to two weeks, antibody penetration and tissue labeling dramatically improved. When incubated for a longer time period, antibodies were able to penetrate deeper into the brain. We estimated penetration into the brain of at least 1mm after one month of staining. Labeling with anti-acetylated tubulin in the adult brain reveals neuronal cell bodies along the diencephalic ventricle after two weeks in both primary and secondary antibody (Figure 2.4A). The acetylated tubulin antibody labels a stabilized or acetylated form of tubulin found in embryonic axons, but in the adult brain appears to label only neuronal cell bodies, as axonal projections are not seen (Figure 2.4B). A schematic side view with the location of the section, as well as a representative schematic transverse section from an adult neuroanatomical atlas, depicts the location of these neuronal cells in the adult brain (Figure 2.4C; Wullimann et al., 1996).

The major obstacle for whole brain labeling is antibody penetration, which is affected by both the thickness of the polymerized hydrogel surrounding the brain and the thickness of the brain itself. By reducing excess gel around the brain and increasing incubation times in primary and secondary antibody, we will be able to label deeper structures in the adult brain. While our

antibody labeling protocol proved to be efficient up to 1mm with primary and secondary incubations of 2 weeks each, this can be improved with longer incubation times. We also found that our technique produced an accumulation of antibody within the polymerized hydrogel surrounding the brain (Figure 2.4A). We are now trying to minimize this, as well as speed up the antibody labeling of deeper brain structures, by driving the primary and secondary antibody into the brain with an electric current similar to the active clearing process. We are also experimenting with alternative clearing methods that will create a porous hydrogel network that will be more easily penetrated by antibodies (personal communication with Dr. Joseph Bergan).

D. Discussion

i. Generating and imaging transparent adult brain tissue for the atlas

We have generated a 3-Dimensional expression atlas of the adult zebrafish brain using intact, transparent brain tissue imaged with FLSM. High resolution images indicate that our protocol results in proper fixation, polymerization, lipid clearing, and refractive index homogenization of adult brain tissue. Transparent brains from different transgenic lines displayed bright and clear expression patterns that were comparable to the expression patterns observed in sectioned tissue. Image acquisition using FLSM is fast and each whole brain images were acquired in less than five minutes. A 3-Dimensional image of the entire brain can then be created, which allows detailed analysis of expression patterns in any plane and replaces the need for manual tissue sectioning. However, while this protocol produces robust and structurally sound brain tissue that displays transgene expression accurately in the brain, there are some areas of the protocol that can be improved.

We discovered fixed brain tissue produced highly autofluorescent blood vessels in all channels during imaging. Autofluorescence may be a desirable attribute in identifying brain regions, as blood vessels have been shown to be conserved, and may be used as an important landmark in the creation of the reference brain. However, autofluorescent blood vessels may interfere with or reduce the clarity of expression data in the brain. The appearance of blood vessels may be reduced with perfusion fixation, which has been successful in mouse. This would also serve as a more efficient method of fixation as it would carry hydrogel to the brain via vasculature, as well as clear blood remaining in the vessels. Additionally, autofluorescence in blood vessels may be subtracted during image processing using Image J or similar imaging software.

We are currently trouble-shooting the inconsistent preservation of fluorescence in prepared brain tissue. The loss of fluorescence in >80% of brains through the dissection and tissue preparation process is incompatible with the high-throughput goals of this project. Further experiments are needed to uncover the issue in our current tissue preparation pipeline. A major difference between zebrafish and mouse brain preparations is that mouse brains are perfusion-fixed, which ensures rapid tissue fixation. For practical reasons and challenges with perfusing zebrafish, we do not perfusion-fix zebrafish brains. Instead our current fixation method entails rapid dissection in cold PBS followed by immersion in cold hydrogel. It is possible that cell lysis and protein degradation during dissection affects fluorescence levels. We will continue to optimize our fixation method, including new attempts at perfusion fixation.

Another improvement would be to generate a more efficient method of polymerizing the hydrogel and brain tissue. So far we have generated a plexiglass mold that facilitates alignment of dissected brains in hydrogel prior to polymerization. The brains may then be cut from this

sheet using a razor blade, producing a block of hydrogel around the brain, which is optimal for imaging with FLSM. While this has been effective, a compartmentalized mold may be useful for separating brains from different lines. However, compartmentalizing has proved to be a challenge as polymerization is not effective around right corners or at volumes below 250µl.

For optimal imaging of transparent brain tissue with FLSM it is important to keep the hydrogel block surrounding the brain clean and free of bubbles, to use only a small amount of glue that will not interfere with imaging when mounting the magnet, to use Optiview at RI=1.45, and to keep the panels in the imaging chamber clean. To account for less intense fluorescent proteins, like mCherry, a 20x lens may be used. Data obtained with a 20x lens can be stitched together post imaging. The mCherry fluorescent protein may be enhanced with antibody labeling, but the use of fluorescence lines with dTomato may be more useful based on its higher intensity.

ii. Value of an adult brain atlas to the zebrafish community

The Zebrafish Adult Brain Browser (ZABB) provides a powerful tool for neuroscience research that current atlases cannot offer. We have the ability to generate and image intact, transparent adult brains from fluorescent transgenic lines and incorporate expression data onto an annotated reference brain image. This will enable us to compare the relative expression patterns of proteins and molecules of interest and observe their location within the brain and different cell types. A large number of transgenic lines and antibodies are currently available for zebrafish, which alone could provide a wealth of information regarding molecular mechanisms and connectivity within the brain.

Applications for the ZABB range from descriptive to functional and may be useful for a variety of studies focused on adult zebrafish brain function. The descriptive aspect of the atlas may be important for identifying sex differences in both anatomy and gene expression, visualizing the progression of the aging brain, and observing and tracing neural connections within the brain. The ability to map activity post-hoc using anti-pERK antibodies would provide a functional aspect to the atlas and allow the visualization of neural mechanisms associated with simple and complex behaviors (Randlett et al., 2015). With an increasing interest in regeneration in the adult zebrafish nervous system, this atlas could be used to document proliferation rates throughout the life of the fish and could help identify how signaling systems in teleost brains maintain proliferative potential into adulthood (Reimer et al., 2009). This atlas may also be used to compare gene expression patterns in healthy fish to older or diseased fish, which may help to identify or rule out certain signaling systems in these processes. The relatively small size of adult zebrafish allows data to be generated, analyzed, and imaged rapidly, unlike larger model systems. By incorporating other model species into the atlas, comparisons between vertebrate species can be made. This work is the beginning of an adult zebrafish brain atlas that will serve as an important tool for the zebrafish community and have potential clinical significance. By developing a better understanding of the adult nervous system at a functional level we may uncover unknown aspects of neural function and provide better methods for treating a wide variety of diseases caused by neural dysfunction.

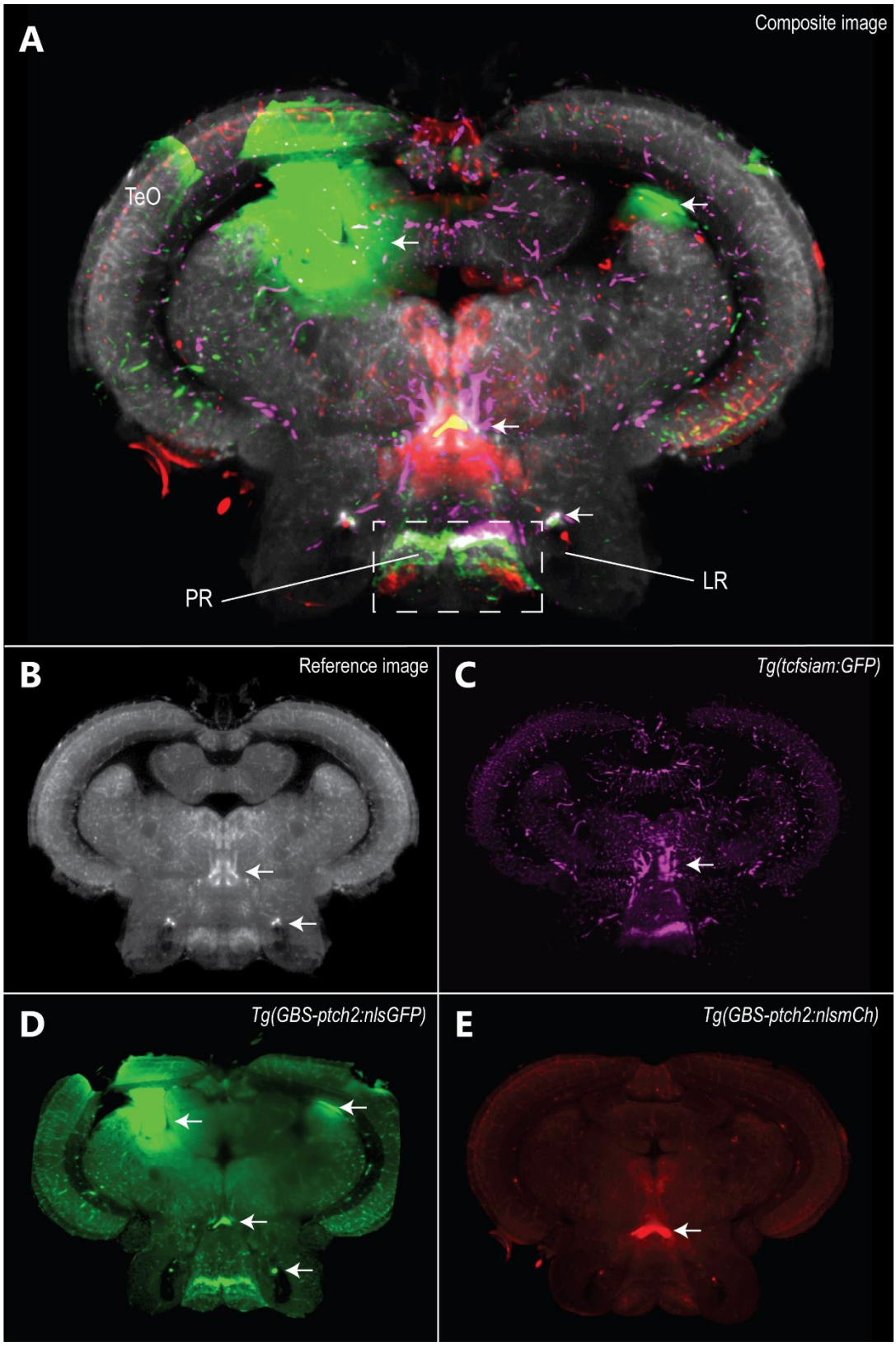
A
Composite image
TeO
PR
LR
B
Reference image
C
Tg(tcfsiam:GFP)
D
Tg(GBS-ptch2:nlsGFP)
E
Tg(GBS-ptch2:nlsmCh)

Figure 2.1: Fluorescent expression patterns from three transgenic lines were aligned and mapped onto a reference brain. A) A composite transverse image of the reference brain (gray) with the expression patterns from three transgenic lines, including *Tg(tcfsiam:GFP)* (magenta), *Tg(GBS-ptch2:nlsGFP)* (green), and *Tg(GBS-ptch2:nlsmCh)* (red). Areas of autofluorescence are indicated with white arrows, besides widespread autofluorescent blood vessels. Rectangular box indicates gene expression data along the PR from the three lines. (PR: posterior recess, LR: lateral recess) B) Reference brain image (gray). C) Expression of Wnt-responsive cells (magenta) from the line *Tg(tcfsiam:GFP).* D) Expression of Hh responsive cell nuclei (green) from the line *Tg(GBS-ptch2:nlsGFP).* Strong autofluorescence is observed in the left and right dorsal regions of the tectum. D) Expression of Hh responsive cells (red) from the line *Tg(GBS-ptch2:nlsmCh).*

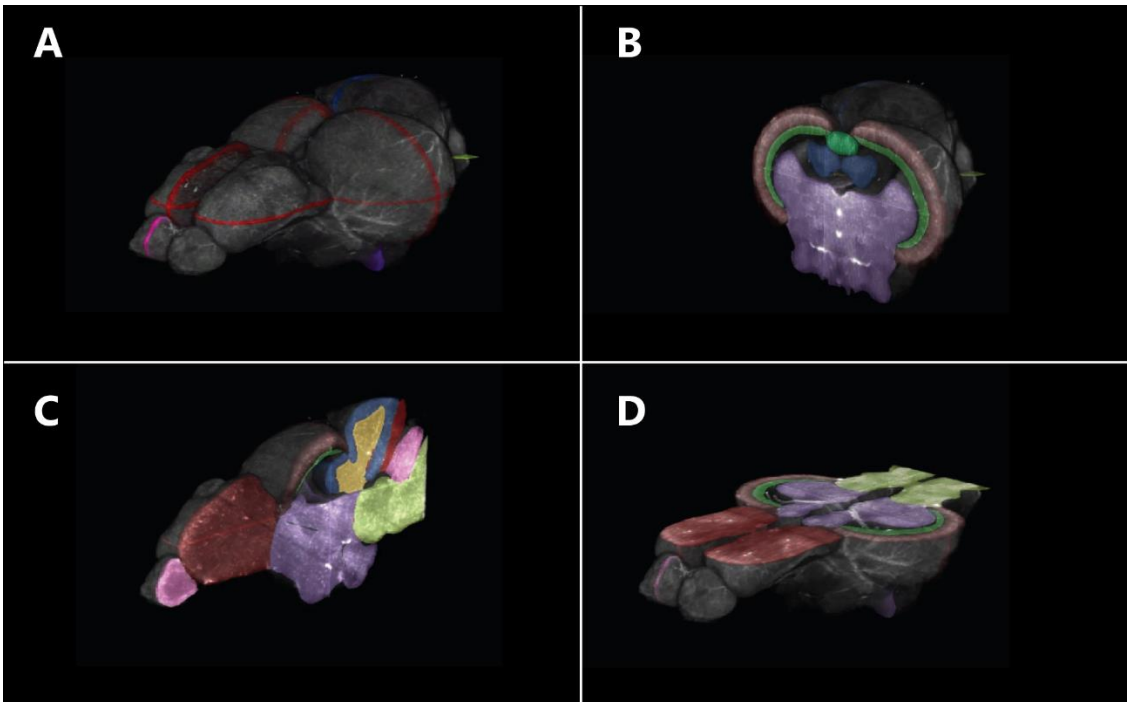

Figure 2.2: Color-coded anatomical annotations of major brain regions on a reference brain. A) Three-Dimensional view of the reference brain with approximate location of sections used for anatomical annotation. Brain structures have been annotated using ZFIN neuroanatomical terms and ontology codes in the B) transverse, C) sagittal, and D) horizontal planes with color-coded values assigned in Image J. Pink; Olfactory bulb (OB, ZFIN# 000402), Dark Red; Telencephalon (Tel, ZFIN# 0000079), Red/Grey; Optic tectum (TeO, ZFIN# 0000445), Dark Green; Periventricular grey zone of the optic tectum (PVG, ZFIN# 0000516), Dark Green; Torus longitudinalis (TL, ZFIN# 0000449), Blue; Valvula cerebelli (Va, ZFIN# 0000603), Purple; mid-ventral Mesencephalon/ Diencephalon (Mes, ZFIN# 0000128/ Di, ZFIN# 0000101), Orange; Cerebellar corpus (CCe, ZFIN# 0000188), Red; caudal lobe of cerebellum (LCa, ZFIN# 0000388) Pink; Cerebellar crest (CC, ZFIN# 0000636), Light green; Medulla oblongata/ Spinal cord (MO, ZFIN# 0021580/ MS, ZFIN # 0000075).

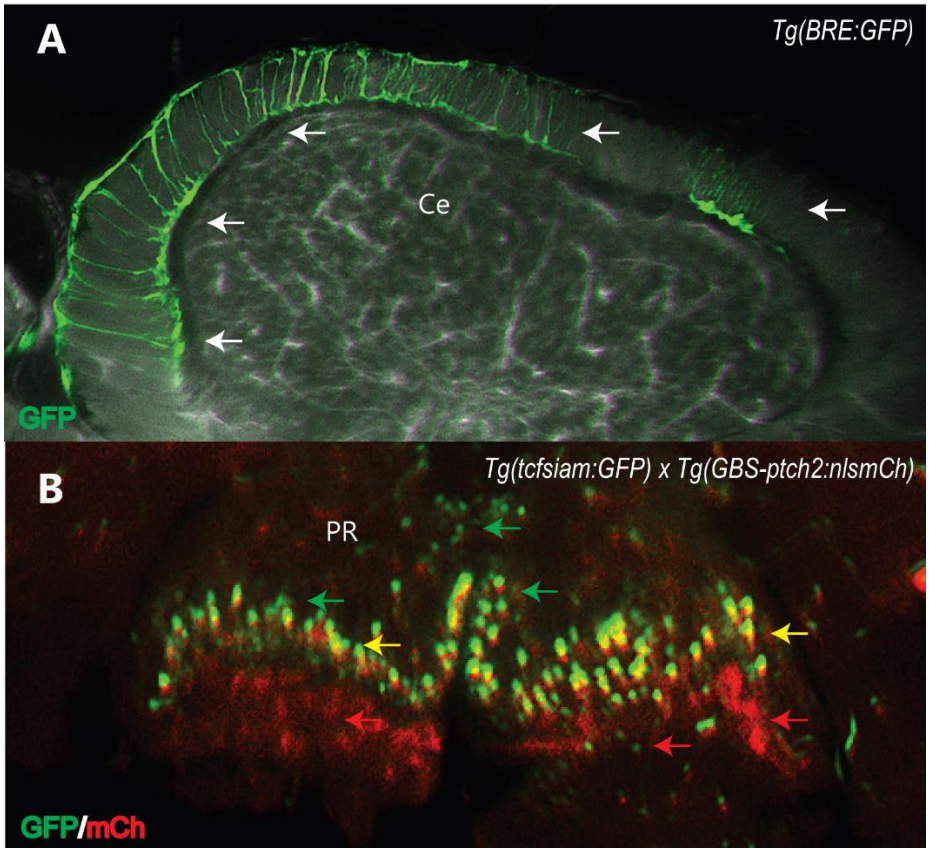

Figure 2.3: Cell morphology and type are observed in structurally maintained whole adult zebrafish brains with FLSM. A) BMP responsive cell projections (green) indicated by arrows within the caudal lobe of the cerebellum (Ce) from the transgenic line *Tg(bre:GFP).* B) Wnt responsive cells (green) and Hh responsive cell nuclei (red) are distinct in the posterior recess (PR) of the diencephalic ventricle from the double transgenic *Tg(GBS-ptch2:nlsmCh x tcfsiam:gf*p).

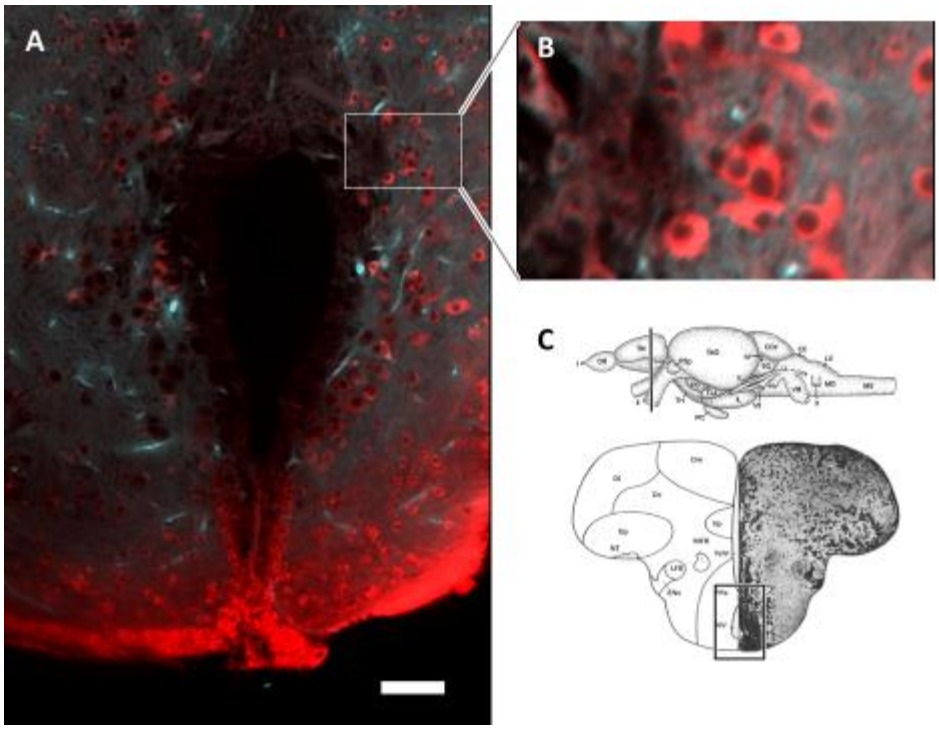

Figure 2.4: Antibody labeling of neurons with anti-acetylated tubulin was achieved up to 1mm into whole adult brain tissue following two week incubations in primary and secondary antibody. A) Neuronal cell bodies (red) labeled with anti-acetylated tubulin primary antibody and Alexa 546 secondary antibody are seen along the anterior diencephalic ventricle. B) Close up view of neuronal cell bodies (red) located beside the ventricle. C) (Top) Approximate location of the section where neuronal cell labeling was observed in panel A in a schematic external side view of the adult zebrafish brain. (Bottom) Representative schematic transverse section with the anterior diencephalic ventricle indicated with a box (Wullimann et al., 1996).

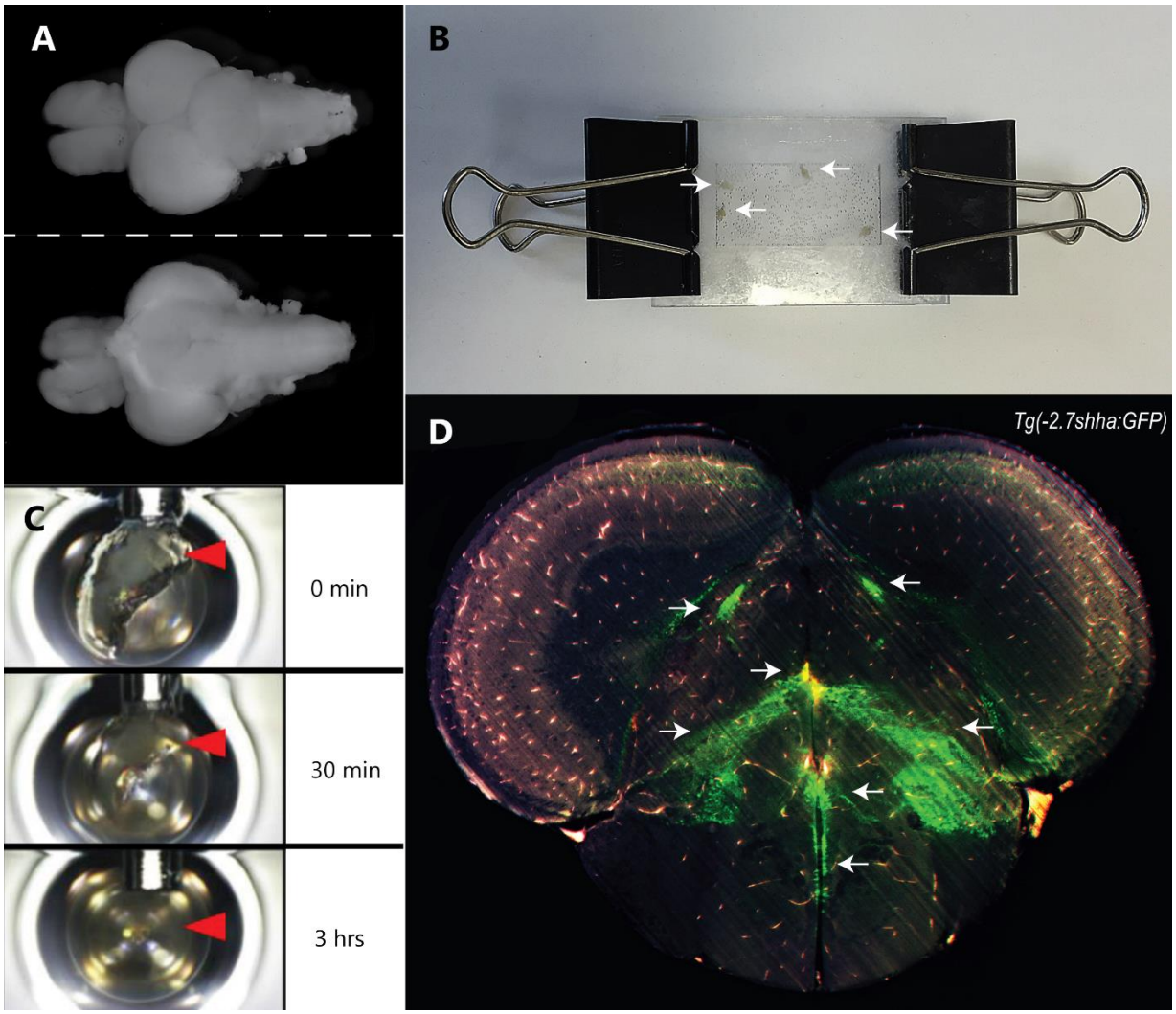

Figure S2.1: A new technique for producing clarified tissue generates transparent, intact adult zebrafish brains that can be imaged using FLSM. A) (Top) Dorsal-view and (Bottom) ventral-view of a dissected adult zebrafish brain. B) Fiberglass mold used to polymerize fixed brain tissue. Polymerized adult brains are indicated by white arrows. C) A hydrogel polymerized adult brain affixed to a magnet in the light sheet imaging chamber (indicated by red arrowheads) becomes transparent in light when placed in Optiview for 3 hours at room temperature. (Top) The brain can be observed with light when first placed in Optiview. (Middle) At 30 mins, the brain is less visible with light. (Bottom) Within 3 hours the entire adult zebrafish brain becomes transparent in light. D) Single z-stack image in the transverse plane at the anterior midbrain of an adult brain from the transgenic line *Tg(-2.7shha:GFP)*. Sonic Hedgehog (Shh) producing cells and cell projections (green) are indicated by white arrows.

Transgenic Line	Reports/Marks	Expression in frozen section?	Expression on Light Sheet (5x)?	Expression on Light Sheet (20x)?	Reference
Tg(-2.7shha:GFP)	Shh secreting cells	Y	Y	-	(Neumann & Nuesslein-Volhard, 2000)
Tg(GBS-ptch2:GFP)	Hh response, cytoplasm	Y (in ventral diencephalon)	N	Y	(Shen et al., 2013)
Tg(GBS-ptch2:nlsGFP)	Hh response, nuclear	Y	Y	-	(Shen et al., 2013)
Tg(GBS-ptch2:GFP-CAAX)	Hh response, membranes	N	N	?	(Shen et al., 2013)
Tg(GBS-ptch2:nlsmCh)	Hh response, nuclear	Y	Y	Y	(Shen et al., 2013)
Tg(GBS-ptch2:mCh-CAAX)	Hh response, membranes	N	N	-	(Shen et al., 2013)
Tg(tcfsiam:GFP)	Wnt response	Y (in blood vessels)	Y (in blood vessels)	Y (in blood vessels)	(Moro et al., 2012)
Tg(dusp6:GFP)	Fgf response	N	N	?	(Akerberg et al., 2014)
Tg(bmp:GFP)	Bmp/TGF-ß response	Y	Y	-	(Collery & Link, 2011)
Tg(rare:GFP)	Retinoic Acid response	N	N	?	(Waxman & Yelon, 2011)
Tg(tp1:bglob:GFP)^{um14}	Notch response	N	N	?	(Parsons et al., 2009)
Tg(nestin:GFP)	Slow cycling neural progenitors	Y	Y	-	(Lam et al., 2009)
Tg(gfap:GFP)	Radial glia	Y	Y	-	(Nuesslein-Volhard & Dahm, 2002)
Tg(olig2:dsRed)	Oligodendrocytes	Y	?	?	(Shin et al., 2003)
Tg(HuC:GFP)	All neurons	N	?	?	(Park et al., 2000)

Table S2.1: Fifteen preliminary transgenic lines were assessed for incorporation into the Zebrafish Adult Brain Browser (ZABB). From left to right: This chart displays a column of fifteen transgenic lines that were candidates for integration into the atlas. Each row provides information for a specific line, including the cell type expressed by the line, whether expression has been observed in frozen sections of the adult brain, whether expression has been observed at 5x or 20x using FLSM, as well as a reference for the transgenic line.

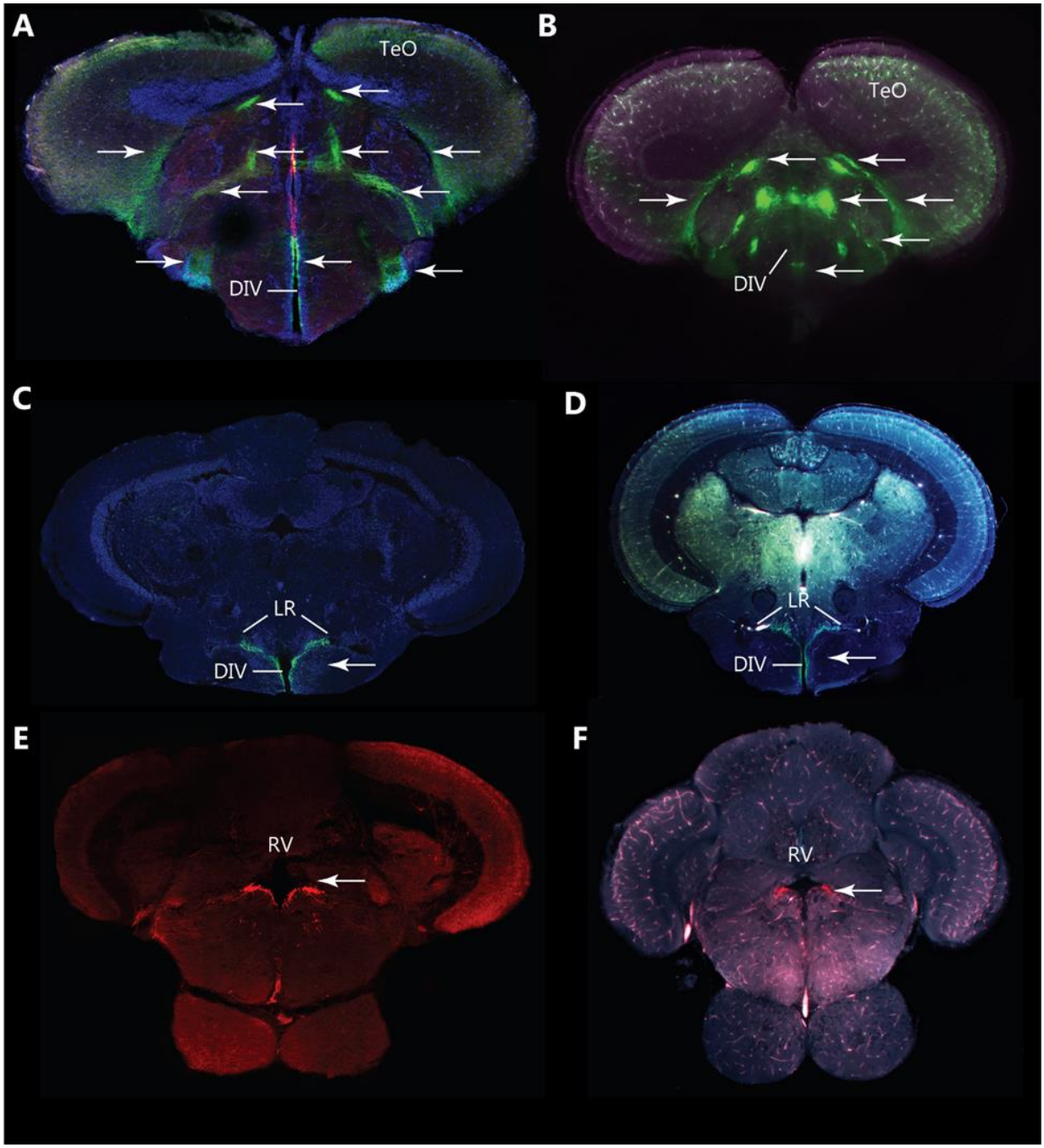

Figure S2.2: Transparent adult brain tissue imaged using FLSM produces comparable expression patterns to sectioned brain tissue, but has decreased sensitivity to fluorescent proteins. A) Frozen transverse section of *Tg(-2.7shha:GFP)* with Hh producing cells (green) observed along the diencephalic ventricle (DIV), in bilateral projections ventro-medial to the optic tectum (TeO), extending from the dorsal DIV to the lateral hypothalamus, and in medial vertical projections dorsal to the lateral projections extending from the DIV. Cell nuclei stained with DAPI are seen in blue. B) Comparable transverse z-stack image of transparent brain tissue from *Tg(-2.7shha:GFP)* generating a similar expression pattern. C) Frozen transverse section of *Tg(GBS-ptch2nlsGFP)* with Hh responding cells (green) located along the DIV and the lateral recess (LR) of the DIV. Cell nuclei stained with DAPI are seen in blue. D) Comparable

transverse slice of transparent brain tissue from *Tg(GBS-ptch2nlsGFP)* also showing Hh responsive cell nuclei (green) along the DIV and LR of the DIV. c) Frozen transverse section of *Tg(GBS-ptch2nlsmCh)* with Hh responsive cell nuclei (red) located ventral to the rhombencephalic ventricle (RV). F) Comparable transverse slice of transparent brain tissue from *Tg(GBS-ptch2nlsmCh*) with Hh responsive cell nuclei (red) in the same region ventral to the RV.

CHAPTER 3

AN ATLAS OF HEDGEHOG MEDIATED CELL-CELL SIGNALING WITHIN PROLIFERATIVE ZONES IN ADULT ZEBRAFISH BRAINS

A. Introduction

i. Neurogenesis in the adult mammalian and teleost brain

The generation of new neurons in the mammalian brain was long thought to occur only during embryonic development. However, in the 1960's a new technique for labeling dividing cells using [H3]-thymidine revealed the generation of neurons in the dentate gyrus of the hippocampus, neocortex, and olfactory bulbs of adult rats (Altman and Das, 1965; Altman and Das, 1966; Altman 1969). Since then immunohistochemical labeling of dividing cells with antibodies, like proliferative cell nuclear antigen (PCNA), as well as bromodeoxyuridine (BrdU), a thymidine analogue that is incorporated into DNA during the S-phase of the cell cycle, have greatly expanded our understanding of adult neurogenesis (Ming and Song, 2005).

In adult mammals, neurogenesis has been extensively studied in the subventricular zone (SVZ) of the forebrain lateral ventricle and the subgranular zone (SGZ) of the dentate gyrus in the hippocampus (Figure 3.1A, Zhao et al., 2008). The SVZ generates olfactory bulb interneurons via the rostral migratory stream (RMS), while the SGZ generates hippocampal granular neurons (Chapouton et al., 2007). While neurogenesis does exist outside of the SVZ and SGZ in areas of the basal forebrain, striatum, amygdala, substrantia nigra, subcortical white matter, and the hypothalamus, these regions have received less interest, because *in vivo* levels of dividing cells are much lower (Lee and Blackshaw, 2014). However, lower levels of observed neurogenesis may point to detection issues with current labeling techniques. For instance, the SVZ and SGZ may be more permeable to BrdU than deeper or less vascularized brain regions. It

is also important to note that brain regions with less observed neurogenic activity or with shorter neurogenic windows compared to the SVZ and SGZ may have vital physiological roles. For example, low levels of neurogenesis have been detected in the hypothalamus with BrdU labeling, however the new neurons formed may play important roles in the regulation of metabolism, weight, and energy balance (Kokoeva et al., 2007).

Unlike mammals, teleost fish continue to grow throughout life, and not surprisingly show more widespread neurogenesis as adults. The zebrafish (*Danio rerio*) is an excellent model system for studying neurogenesis in adults based on the conservation of brain structures among vertebrates, the short time period to sexually maturity (adulthood), and presence of sixteen known proliferative zones that remain active in the brain throughout adulthood (Figure 3.1B, Grandel et al., 2006). In this study we utilized zebrafish as a model to investigate the molecular mechanisms behind adult neurogenesis.

ii. Neural progenitor/stem cell regulation

Proliferative zones in the adult mammalian and teleost brain are neurogenic niches that contain neural progenitor cells capable of self-renewal and giving rise to a wide variety of differentiated neuronal and glial subtypes (Grandel et al., 2006). In mammals, the ventricular-subventricular zone (V-SVZ) of the forebrain lateral ventricle is a neurogenic niche that contains astroglial-like cells, known as B1 cells, which have morphological similarities to embryonic radial glia and act as adult neural stem cells (NSCs) (reviewed in Lim and Alvarez-Buylla, 2014). B1 cells may represent the small percentage of mammalian embryonic radial glia that retain NSC potential after differentiating into astrocytes in adulthood (reviewed in Schmidt et al, 2013). In teleosts, such as zebrafish, radial glia persist into adulthood and continue to serve as NSCs (Grandel et al.,2006; Adolf et al., 2006; Lam et al., 2009; Ganz et al., 2010; März et al.,

2010). Thus, it is possible that the life-long neurogenesis observed in the adult zebrafish brain is due to the widespread retention of embryonic radial glial cell characteristics. It also points to the differentiation of radial glia into astrocytes as a possible explanation for the loss of NSC potential that is observed in adult mammals.

Progenitor cells in the adult brain are characterized based on their proliferative potential. In mammals and fish, quiescent or non-dividing NSCs are known as B1 cells and Type I cells respectively (Figure 3.2). In mammals, B1 cells are activated into proliferative B1a cells, which transition into C cells or transit amplifying cells (TACs) that divide symmetrically three times before becoming migratory neuroblasts, known as A cells (Figure 3.2A; reviewed in Lim and Alvarez-Buylla, 2014). A cells travel along the rostral migratory stream (RMS) to the olfactory bulbs and differentiate into olfactory bulb interneurons. The ability of newly generated cells to migrate out of their site of origination reveals the importance of neurogenesis for the entire brain and shows that it is not limited to brain proliferative zones.

In fish, quiescent Type I cells become activated into proliferative (slow cycling) Type II cells, which may then divide symmetrically and self-renew or divide asymmetrically and generate Type III TACs, which are fast dividing cells that can produce other TACs or become specialized neuroblasts or glioblasts (Figure 3.2B). In both mammals and fish, quiescent and activated NSCs express glial cell markers (i.e. GFAP, GLAST, BLBP, and s100b), indicating NSCs from both models share glial cell characteristics. Actively proliferating NSCs label with proliferative cell markers, such as PCNA and BrdU, and neuroblasts/glioblasts express markers indicating commitment to a specific cell types (i.e. the neuronal cell marker *ascl1*). Mammalian and teleost NSC models (Figure 3.2) follow a similar pattern where quiescent NSCs are activated to begin dividing and then may generate differentiated neuronal or glial cells (fish) or may pass

through a fast diving or transit amplifying phase before differentiating (mammals and fish). Either path to the formation of new cells is orchestrated by complicated molecular communication within the brain that is not entirely understood. In mammals, neural regulation is shown to be activity dependent in olfactory neuron populations, indicating the importance of behavioral and environmental effects on neurogenesis as well (Santoro and Dulac, 2012).

Several signaling pathways are implicated in regulating NSC proliferation, self-renewal, and differentiation in both mammals and fish, including the Notch, Wnt, Retinoic acid (RA), Fibroblast growth factor (Fgf), Bone morphogenetic protein (Bmp), and Sonic Hedgehog (Shh) signaling pathways (Figure 3.2B, reviewed in Schmidt et al., 2013; Chapouton et al., 2010; Shi et al., 2009; Chapouton et al., 2007). The Notch signaling pathway is thought to maintain and return NSCs to a quiescent state, while the Wnt, Fgf, Bmp, and Shh signaling pathways are thought to activate proliferative NSCs (Figure 3.2B). The RA and Shh signaling pathways may be important in the transition of slow cycling Type II cells to Type III TACs (Figure 3.2B). We are interested in understanding the role of Shh signaling in the regulation of neural progenitor cell proliferation in the adult brain.

iii. Hedgehog signaling and adult neural stem cell regulation

Hedgehog (Hh) belongs to a family of evolutionarily conserved, secreted proteins that play key roles in embryonic development, adult tissue homeostasis, and stem cell proliferation (reviewed in Schmidt et al., 2013). During development Hh acts as a morphogen to regulate cell fate and pattern embryos in a dose-dependent manner (reviewed in Ingham and McMahon, 2001). In adults Hh continues to play a role by regulating tissue plasticity, maintenance, and repair, as well as neural progenitor cell populations (reviewed in Petrova and Joyner, 2014; Martinez et al, 2013). In mammals, Shh induces both the proliferation of stem cells and the

generation of astrocytes, greatly increasing neurogenesis and cell survival. Blocking Shh reduces cell proliferation, differentiation, and survival (Araújo et al., 2014). Somatic mutations that cause increased Hh signaling are associated with human neural tumors including glioblastomas and medulloblatomas, suggesting Hh can act as a potent mitogen in the adult (reviewed in Lim and Alvarez-Buylla, 2014).

In adult mammals, Shh plays an important role in the proliferative potential of B1 cells in the V-SVZ (Ihrie et al., 2011). While the mechanism of Shh signaling is unknown, several characteristic features of B1 cells suggest possibilities. B1 cells have apical processes that reach toward the pial surface of the ventricle and end-feet that are located on blood vessels, both features shared by embryonic radial glia, as well as a single primary cilium facing the ventricular lumen (Figure 3.3A, reviewed in Lim and Alvarez-Buylla, 2014). The presence of a primary cilium, which is necessary for Shh signaling in early neural precursors as well as in adults, may indicate a possible route for Shh to communicate with B1 cells (Wong and Reiter, 2008; Briscoe and Therond, 2013). A variety of signaling proteins, including Shh, can also circulate in cerebral spinal fluid (CSF) throughout the brain ventricles, potentially providing a direct route for Shh to communicate with B1 cells and activate their NSC potential. Insulin-like growth factor 2 (IGF-2) has been shown to communicate with B1 cells via CSF, indicating that activation through this route is a possibility (Lehtinen et al., 2011). Overall the mammalian NSCs or B1 cells are Hh responsive radial glial-like cells found lining the ventricle.

While Shh plays key roles in zebrafish development, less is known about its role in the adult nervous system. Recent work indicates Hh may be partially responsible for the remarkable regenerative capacity of the zebrafish spinal cord, as Hh signaling is upregulated in the ventral spinal cord following spinal cord lesion (Reimer et al., 2009). Shh also continues to be expressed

in the adult zebrafish brain, but little is known of the cell types or brain regions that retain Hh signaling or how Hh may affect adult neurogenesis (reviewed in Schmidt et al., 2013). Hh responsive cells in the adult zebrafish hypothalamus have been shown to be proliferative radial glia that contact the ventricular surface, similar to B1 cell in the V-SVZ in mammals (Figure 3.3B, unpublished data from the Karlstrom lab). Hh responsive cells may receive a signal from nearby Shh producing cells or by interacting with signaling proteins present in CSF (Figure 3.3B). Both Shh and Wnt responsive cells have been identified along the posterior recess of the diencephalic ventricle in adult zebrafish, which may indicate a potential neurogenic role for both signaling proteins in the hypothalamus (Figure 3.3B).

Given the importance of Hh signaling in mammals and the establishment of zebrafish as a new model for adult neurogenesis, we undertook a systematic analysis of Hh signaling in the adult zebrafish brain with the goal of providing the first complete description of Hh responsive regions and cell types. The creation of a detailed atlas of Hh signaling was accomplished with sectioned and antibody labeled adult brain tissue, as well as whole brain imaging of cleared brain tissue generated using a protocol similar to CLARITY (Chung and Deisseroth, 2013; Tomer et al., 2014), from transgenic zebrafish Hh reporter lines. This atlas could potentially help guide studies on the mechanism of Hh in NSC regulation and may contribute to new therapies for neurodegenerative disorders and cancers.

B. Methods

i. Maintenance and growth conditions

Zebrafish were kept in a 14 hour light/ 10 hour dark cycle at 28°C. Growth conditions were standardized by maintaining a density of ~30 fish per 3L tank and a single regularly scheduled daily feeding.

ii. Zebrafish transgenic lines

We utilized the following transgenic lines, *Tg(GBS-ptch2:nlsmCh),* and *Tg(GBS-ptch2:nlsGFP),* to report Hh responsive cells in the adult zebrafish brain (Shen et al., 2013). These lines contain a ~1.2kb *GBS-GBS-ptch2* DNA regulatory element that drives transgene expression in the nuclei of cells responding to Hh signaling. Adult zebrafish between 3 and 6 months of age were selected for this study. The standard length of fish across these ages is as follows: 3mpf: SL 20 ±2mm, 6mpf: SL 30 ±2mm. Sex was recorded to account for sexually dimorphic differences.

iii. Euthanization and tissue preparation

Zebrafish were euthanized in a lethal dose of MS-222. Fish were then placed in a petri dish of ice-cold PBS for decapitation or brain dissection. For sectioning, fish were decapitated and stored in 4% PFA overnight at 4°C. The skull cap and jaw were removed to allow adequate fixation of the brain. Following fixation, heads were placed in an embedding media (1.5% agar, 5% sucrose) and cryoprotected in a solution of 30% sucrose at 4°C. The embedded samples were sectioned (20-30µm) using a Leica CM1850 cryostat. For whole brain imaging, dissected brains were prepared following a protocol adapted in mouse (Menegas et al., 2015).

iv. *In situ* hybridization and immunohistochemistry

In situ hybridization was performed on transverse sections of 3-month old (SL = 20 ±2mm) wild-type fish using a *ptch2* digoxigenin probe. Antibody labeling was performed on

transverse sections of 3-6 month old (SL = 20-30mm) zebrafish from the Hh reporter lines, *Tg(GBS-ptch2:nlsmCh),* and *Tg(GBS-ptch2:nlsGFP).* Primary antibodies included anti-PCNA mouse/IgG2a 1:500 (Sigma p8825), anti-GFP rabbit/IgG 1:500 (Torrey Pines), anti-RFP (mCherry) rabbit 1:500 (MBL pm005). Secondary antibodies included goat-anti-mouse IgG2a Alexa 647 1:800 (A221241), goat-anti-rabbit IgG Alexa 488 1:800 (A11008), and goat-anti-rabbit IgG Alexa 546 1:800 (A11010). Frozen sections were dried 24 hours prior to antibody labeling.

v. Confocal microscopy

Transverse brain cryosections were cover slipped with Aquapolymount and imaged with a Zeiss LSM 700 confocal microscope. Brain regions were identified using a published atlas of adult zebrafish neuroanatomy (Wullimann et al., 1996).

vi. Fluorescent light sheet microscopy (FLSM)

Whole brains were imaged in a Zeiss Light Sheet Microscope at 5x and 20x. Prior to imaging, brains were placed in Optiview (patent pending), a refractive index matching solution that renders the brain transparent. An adult zebrafish atlas was generated using Image J, Elastix software, and MatLab scripts previously used to create a mouse reference brain atlas (Klein et al., 2010; Menegas et al., 2015).

C. Results

i. Fluorescent reporter lines reveal Hh responsive cells in the adult hypothalamus

Six transgenic reporter lines that express GFP or mCherry under the control of a 1.2kb promoter region from the *ptch2* Hh target gene were used to identify nuclei (*Tg(GBS-*

ptch2:nlsGFP) and *Tg(GBS-ptch2:nlsmCh)*), membranes (*Tg(GBS-ptch2:GFP-CAAX)* and *Tg(GBS-ptch2:mCh-CAAX)*), and the cytoplasm (*Tg(GBS-ptch2:GFP)* and *Tg(GBS-ptch2:mCh)*), of Hh responsive cells (Figure 3.4B, Shen et al., 2013). All six lines accurately report the Hh response during embryonic and larval stages, although the relative intensity of the fluorescent protein of each line differs in larvae (Figure 3.4B; Shen et al., 2013; Shen and Karlstrom unpublished data). In 4dpf larval zebrafish, the relative intensity of the GFP expressing lines was nuclear-GFP > cytoplasmic-GFP > membrane-GFP, and for the mCherry expressing lines was membrane-mCherry > nuclear-mCherry = cytoplasmic-mCherry (Figure 3.4B). However, only four of the six lines continue to express fluorescent proteins in the adult brain, as seen in sagittal sections through the ventral hypothalamus (Figure 3.5). Table 3.1 lists the official and abbreviated nomenclature for each transgenic line, as well as the sub-cellular labeling, relative fluorescent intensity of 4dpf larvae, and the stages (embryos, larvae, or adults) expressed by the six Hh reporter lines.

To show these transgenic lines accurately report *ptch2* expression, we compared fluorescent protein expression to *ptch2* mRNA expression, as visualized by *in situ* hybridization (ISH) using a *ptch2* antisense mRNA probe. We found that nuclear-GFP and nuclear-mCherry most faithfully recapitulated *ptch2* mRNA expression as visualized by ISH, while the expression patterns observed in the membrane-mCherry and cytoplasmic-GFP lines were more variably aligned with *ptch2* mRNA expression in the adult brain (data not shown). Thus, while all four adult-expressing Hh reporter lines utilize the same 1.2kb *GBS-ptch2* regulatory element, each line reveals only a subset of *ptch2* expressing cells (see next section). Nonetheless, in combination with *ptch2* ISH analysis, these lines allow a more detailed view of the Hh-responsive cell types, allowing quantification of cell number (nuclear-GFP and nuclear-mCherry

lines) and providing information of cell morphology (membrane and cytoplasmic lines) not possible using ISH. Based on the quality of labeling we decided to predominantly use the nuclear-GFP and nuclear-mCherry lines for further analysis of Hh responsive regions in the adult brain. Table 3.1 summarizes the accuracy of Hh reporting in the four transgenic lines with transgene expression in the adult brain.

We compared fluorescent protein expression in sectioned brain tissue from 1-month old (SL = 10 ±1mm; Parichy et al., 2009) fish from the four adult-expressing lines along the lateral recess (LR) and posterior recess (PR) of the diencephalic ventricle (DIV) in the ventral hypothalamus (Figure 3.5). Previous work in the lab has revealed that the Hh responsive cells along the diencephalic ventricular zones are radial glia that remain proliferative in the adult (Figure 3.3B). Both nuclear fluorescent protein expressing reporter lines, nuclear-GFP (Figure 3.5A) and nuclear-mCherry (Figure 3.5B), label the nuclei of Hh responsive cells along the dorsal and ventral regions of the LR, as well as the dorsal region of the PR. Fluorescence is brightest in the nuclear-GFP line in these regions, although nuclei are still visible, though dim, in the nuclear mCherry-line. In membrane-mCherry, the dorsal region of the PR had punctate mCherry expression in a pattern similar to the nuclear lines and diffuse mCherry expression along the dorsal region of the LR (Figure 3.5C). Expression in this line did not reveal either cell morphology or projections, as expected of a membrane-localized fluorescent protein line. Therefore, while the transgene appears to be expressed in the correct location, issues with sub-cellular mCherry localization makes this line less useful as a reporter of the Hh response in the adult hypothalamus. Cytoplasmic-GFP expression reveals cellular projections and morphologies in sectioned tissue, particularly in the PR and ventral hypothalamus near the pituitary gland (Figure 3.5D), and in the pituitary gland itself (data not shown). Strangely, no expression was

observed along the LR in these fish, while expression in the ventral hypothalamus and pituitary were not observed in the nuclear or membrane localized fluorescent protein lines.

ii. Hedgehog responsive cells throughout the adult zebrafish brain in transverse sections

Hh responsive cells were identified in the brain of 3-month old (SL = 20 ±2mm; Parichy et al., 2009) adult zebrafish using *ptch2* mRNA expression, as seen with *in situ* hybridization (ISH), as well as transgene expression from the nuclear-GFP and nuclear-mCherry Hh-reporter lines. Hh responsive brain region are presented in transverse tissue sections moving from anterior to posterior. The expression of *ptch2* mRNA from ISH is presented first in each figure, followed by a schematic transverse section from a published adult neuroanatomical atlas to identify brain regions (Wullimann et al., 1996). We then present transverse images of sectioned and antibody labeled brain tissue, as well as optical sections from whole brains imaged using fluorescent light sheet microscopy (FLSM), from the nuclear Hh reporter lines. Each image contains a schematic external side view of the adult brain showing the approximate location of the section. We determined which lines were useful for representing Hh signaling in different brain regions based on the lines ability to recapitulate *ptch2* mRNA expression as seen with ISH. We also discovered brain regions, both proliferative and non-proliferative zones, which respond to Hh signaling in adult zebrafish brains.

a. Hedgehog responsive cells in the olfactory bulbs and at the olfactory bulb and dorsal telencephalon border

Hh responsive cells are found within the olfactory bulbs (OBs) and in the proliferative zone at the OBs and dorsal telencephalon (D) border. While the OBs are not a proliferative zone, they often contain proliferative cells that migrate along a rostral migratory stream (RMS) from the proliferative zones at the OBs and D and ventral telencephalon (Tel). In the olfactory bulbs,

ptch2 mRNA is expressed in a small subset of cells in the internal cellular layer (ICL) and external cellular layers (ECL) of the internal region of the OBs and in a few cells along the peripheral region of the OBs in the glomerular cell layer (GL) (Figure 3.6A). The expression of *ptch2* mRNA is sparse in the OBs and is only present in a small percentage of cells (Figure 3.6A). We found that the nuclear-mCherry line recapitulates *ptch2* mRNA expression in the OBs accurately and is a useful line for representing Hh responsive cells in this region. However, transgene expression with the line represents a smaller percentage of cells than with ISH, with sparse nuclei located in the ICL and ECL and only a few nuclei located in the GL (Figure 3.6C). The nuclear-GFP line is not useful for representing Hh responsive cells in the OBs as no GFP expressing nuclei are observed in this region (Figure 3.6D). However, strong background fluorescence found in the OBs, and in particular the GL, of both lines may be hindering the visualization of transgene expressing nuclei in the OBs. We believe the strong fluorescence in the OBs, particularly in the GL, does not represent real expression based on only a few cells expressing *ptch2* mRNA in this region.

In the proliferative zone at the border between the OBs and D, *ptch2* mRNA is expressed in a cluster of cells located along the OB and D border, with a greater percentage of cells expressing *ptch2* near the telencephalic ventricle (TelV) and fewer cells expressing *ptch2* more lateral to the TelV (Figure 3.6E). In the D, *ptch2* mRNA is expressed in a few cells lining the dorsal region of the TelV, along the midline, and in a small subset of cells located in the dorso-lateral region (Figure 3.6E). In the OBs a larger subset of *ptch2* expressing cells were seen in the ICL and ECL, while fewer and more sparse cells were seen in the GL (Figure 3.6E). Neither Hh reporter line is useful for documenting the Hh response in the proliferative zone based on a substantially smaller proportion of cells expressing the transgene compared to cell expressing

ptch2 mRNA with ISH. In the nuclear-mCherry line, a few nuclei express the transgene in disperse locations in D and in the OBs, but do not seem to cluster along the border between the two brain regions (Figure 3.6G). Background fluorescence is also observed in this line in the GL of the OBs, as well as in the ventro-lateral region of the D, which may potentially hinder the visualization of transgene expression (Figure 3.6G). While the nuclear-GFP line did not appear to express GFP in nuclei in the anterior OBs, a greater percentage of transgene expressing nuclei are found in the OBs in this line when compared to the nuclear-mCherry line at the OB and D border (Figure 3.6H). However, no GFP expressing nuclei were found in the D (Figure 3.6H). Additionally, neither of the Hh reporter lines accurately reported *ptch2* mRNA expression along the TelV in the D (Figure 3.6G-H).

Transgene expression in the nuclear-mCherry line is seen in a transparent whole adult brains imaged with FLSM along the OB and D border, as well as in a few nuclei within the OBs (Figure 3.6I). Background fluorescence in the GL of the OBs is also seen in whole-brain imaging of this line (Figure 3.6I). We found that brains imaged with FLSM produced comparable expression patterns to sectioned brain tissue. However, the mCherry fluorescent protein is less intense and is often difficult to observe in certain brain regions, such as the OBs, but may be amplified with whole brain antibody labeling.

b. Hedgehog responsive cells in the dorsal and ventral telencephalon

Hh responsive cells are found in the proliferative zones in the dorsal and ventral telencephalon (Tel). In the telencephalon (Tel), *ptch2* mRNA is expressed in a high percentage of cells along the periphery in the dorsal Tel (D), along D TelV (dTelV), and the dorsal (Vd) and ventral (Vv) regions of the ventral telencephalic ventricle (vTelV), as well as in sparse cell in the dorsal entopenduncular nucleus (End) (Figure 3.6A and 3.7A). Overall, the nuclear-mCherry line

reports *ptch2* mRNA expression in a greater percentage of Hh-responsive regions in the Tel compared to the nuclear-GFP line. Transgene expression in the nuclear-mCherry line is seen in a sparse cells along the d,vTelV and within the End, but in a high percentage of cells within the Vv in both sectioned and transparent brain tissue (Figures 3.7C-D). Transgene expression in the Vv and End closely resemble *ptch2* mRNA expression, but transgene expression along the dTelV and Vd are present in a lower percentage of cells compared to those expressing *ptch2* mRNA (Figures 3.7C-D). In nuclear-GFP, the transgene is expressed in a few sparse cell locate along the d,vTelV, but in a greater percentage of cells located in the Vd in both sectioned and transparent brain tissue (Figure 3.7E-F). Transgene expression in this line only recapitulates *ptch2* mRNA expression in the Vd and does not report expression in the End (Figures 3.7E-F). Additionally, neither Hh-reporter line reports transgene expression along the peripheral D as seen with ISH (Figures 3.7C-F). Therefore, the nuclear-mCherry line most accurately reports Hh responsive cells in the Tel, despite a lower percentage of cells along the dTelV and dorsal Vd. Both the nuclear-mCherry and nuclear-GFP line may be used together to account for cells in the vTelV.

c. Hedgehog responsive cells in the diencephalic ventricular region

Hh responsive cells are found along the diencephalic ventricle (DIV), another proliferative zone in adult zebrafish brains. While there are inconsistencies with transgene expression along the DIV when compared to *ptch2* mRNA expression in both lines, overall the nuclear-GFP line has the brightest fluorescent protein expression along the DIV and is most similar to the expression of *ptch2* mRNA. The nuclear-mCherry line also reports accurate transgene expression in most regions along the DIV, but the expression is relatively weak. Both lines may be used together to account for inconsistencies in transgene expression when

compared to *ptch2* mRNA expression. Overall, we discovered a large population of Hh responsive cells along the DIV, including the lateral (LR) and posterior (PR) recesses.

Beginning in the anterior region of the DIV, *ptch2* mRNA is expressed in several nuclei along the DIV including the anterior thalamic nucleus (A), ventromedial thalamic nucleus (Vm), posterior parvocellular preoptic nucleus (Ppp), and within the ventral hypothalamus (Hv), as well as along the DIV between the ventral habenular nuclei (Hav) (Figure 3.8A). Expression is in a high percentage of cells located close to the DIV. While the nuclear-GFP line accurately reports Hh responsive cells along the DIV, there are some inaccuracies in transgene expression in the anterior-most region. The line expresses its transgene in a lower percentage of cells in all nuclei located along the DIV when compared to the number of cells expressing *ptch2* mRNA along the DIV in sectioned tissue (Figure 3.8E), while no cells appear to express the transgene along the DIV in brains imaged with FLSM (Figure 3.8F). Additionally, nuclear-GFP expresses Hh responsive cell nuclei in two brain regions that do not express *ptch2* mRNA: the region between the ventral (Hav) and dorsal (Had) habenular nuclei in both sectioned and transparent brain tissue (Figure 3.8E-F) and within the ventral optic tract (VOT) in sectioned tissue (Figure 3.8E). Inconsistencies with transgene expression are also observed in the nuclear-mCherry line in sectioned (Figure 3.8C) and transparent (Figure 3.8D) brain tissue where expression is seen in a high percentage of cells along the DIV in only the A and VM, as well as in a few nuclei along the DIV in the Hv (only in sectioned tissue). Nuclear-mCherry accurately reports *ptch2* mRNA expression in a similar number of cells in all regions besides the Hv and Ppp, where a lower percentage of cells express mCherry in the Hv (Figure 3.8C) and no cells express the transgene in nuclei in the Ppp (Figure 3.8C-D).

Along the DIV, *ptch2* mRNA is expressed in a high percentage of cells and in a few dispersed cells within the ventral hypothalamus (Hv) (Figure 3.9A). Transgene expression in the nuclear-GFP line is found in the Hv and the dorsal and ventral aspect of the DIV, as well as surrounding the medial forebrain bundles (MFB) (Figure 3.9E). GFP expressing nuclei along the DIV were more dispersed along the dorsal aspect and located closer to the ventricle along the ventral aspect (Figure 3.9E). GFP expressing nuclei surrounding the MFB did not recapitulate *ptch2* mRNA expression and may be misdirected transgene expression (Figure 3.9E). In FLSM imaging of brains, GFP expressing nuclei were observed in a similar pattern along the dorsal aspect of the DIV, as observed in sectioned tissue, but nuclei were not observed along the ventral aspect of the DIV, Hv, or surrounding the MFB (Figure 3.9F). This lost expression may be regained with whole brain antibody labeling. In nuclear-mCherry, sectioned (Figure 3.9C) and light sheet imaged brains (Figure 3.9D) have transgene expression only along the dorsal aspect of the DIV and not ventrally. Sectioned and antibody labeled brain tissue also show Hh responsive nuclei along medial region of the medial DIV (Figure 3.9C), but these nuclei are not observed in transparent brain tissue (Figure 3.9D).

Moving posteriorly along the DIV, *ptch2* mRNA is expressed along the lateral recess (LR) of the DIV, within the lateral hypothalamic nucleus (LH), and within the medial preglomerular nucleus (PGm) (Figure 3.9G). In sectioned (Figure 3.9K) and light sheet imaged (Figure 3.9L) brains from the nuclear-GFP line, GFP expressing nuclei are observed along the LR of the DIV (with stronger expression along the medial DIV and weaker expression along the LR), as well as a few nuclei in the LH. In sectioned (Figure 3.9I) and light sheet imaged (Figure 3.9J) brains from the nuclear-mCherry line, a small subset of mCherry expressing nuclei were

observed weakly along the LR of the DIV and within the LH. However, transgene expression failed to recapitulate *ptch2* mRNA expression in the PGm in both lines (Figure 3.9I-L).

Along the posterior region of the DIV, *ptch2* mRNA was expressed along the posterior recess (PR) of the DIV in the caudal (Hc) zone of the periventricular hypothalamus and along the LR of the DIV in the dorsal (Hd) zone of the periventricular hypothalamus (Figure 3.9M). In sectioned tissue from nuclear-GFP, GFP expressing cell nuclei are found along the PR of the DIV in the Hc (Figure 3.9Q). This line did not recapitulate *ptch2* mRNA expression along the LR of the DIV in the Hd (Figure 3.9Q). Interestingly, transparent brain tissue from this line did reveal transgene expression along the LR of the DIV in the Hd (Figure 3.9R). In sectioned (Figure 3.9O) and light sheet imaged (Figure 3.9P) brain tissue from the nuclear-mCherry line, mCherry expressing nuclei were observed weakly along the PR of the DIV in the Hc and along the LR of the DIV and in the Hd (Figures 3.9O-P).

d. Hedgehog responsive cells in the optic tectum and cerebellum

Hh responsive cells are found in proliferative zones in the periventricular gray zone (PGZ) of the optic tectum (TeO), at the midbrain-hindbrain border, within the cerebellum, and in the torus longitudinalis (TL). Hh responsive cells are also found in a few disperse cells in the midbrain that are not within a brain proliferative zone. The expression of *ptch2* mRNA is found in a high percentage of cells in the PGZ of the TeO (Figure 3.9A, G, M), at the midbrain-hindbrain border (Figure 3.9M), within the cerebellum (molecular and granular layers of the valvula cerebellum, Val) (Figures 3.9G and M), in the TL (Figure 3.9G) and in a few discreet cells in the midbrain (Figures 3.9A, G, M). Overall, the nuclear-GFP line recapitulates *ptch2* mRNA expression in the PGZ of the TeO, in the Val, and in disperse cells located in the midbrain, while the nuclear-mCherry line recapitulates expression along the midbrain-hindbrain

border and in disperse cells located in the midbrain. Neither line recapitulates *ptch2* mRNA expression in the TL.

In sectioned tissue from the nuclear-GFP line, transgene expression is observed in a small percentage of cells in the PGZ of the TeO (Figures 3.9 E, K, Q) and the Val (Figures 3.9K and Q), as well as in few cells in the midbrain (Figures 3.9E, K, Q). Transgene expression is reported accurately in these regions although it is expressed in a smaller subset of cells than found expressing *ptch2* mRNA. However, transgene expression in the PGZ of the TeO, Val, and in the midbrain is not observed in transparent brain tissue from this line (Figure 3.9F, L, R). This may indicate a loss of transgene expression with this technique, or may suggest the intensity of the GFP expressing nuclei was not strong enough to be detected with a 5x lens. We may be able to regain this expression with whole brain antibody labeling. No transgene expression is observed in the PGZ of the TeO or ValF in the nuclear-mCherry line in both sectioned (Figures 3.9C, I, O) and transparent (Figures 3.9D, J, P) brain tissue. Midbrain nuclei were observed in sectioned tissue from the nuclear-mCherry line (Figure 3.9O), but not in transparent brain tissue (Figures 3.9D, J, P). However, the nuclear-mCherry line does recapitulate *ptch2* mRNA expression along the midbrain-hindbrain border, located ventral to the tectal ventricle (TeV), in both sectioned (Figures 3.9I and O) and transparent (Figures 3.9J and P) brain tissue, unlike the nuclear-GFP line.

e. Hedgehog responsive cells in the hindbrain

In the hindbrain, Hh responsive cell nuclei are found in the proliferative zone along the rhombencephalic ventricle (RV) and in diffuse cells in the hindbrain. Here *ptch2* mRNA is expressed in a high percentage of cells in the in the griseum centrale (GC) along the ventral RV, as well as in a lower percentage of disperse cells in the hindbrain (Figures 3.9M and 3.10A).

Overall, the nuclear-mCherry line best recapitulates *ptch2* mRNA expression in cells in the GC ventral to the RV. Expression is also observed in cells within the medial longitudinal fascicle (MLF), cerebellar crest (CC), caudal lobe of the cerebellum (LCa), and cerebellar corpus (CCe). In sectioned (Figure 3.10C) and transparent (Figure 3.10D) brain tissue from the nuclear-mCherry line, transgene expression is located in diffuse cells in the GC ventral to the RV, which accurately reports *ptch2* mRNA expression (Figure 3.10A). This line also expresses a small percentage of Hh responsive cell nuclei in the MLF, CC, LCa, and CCe in sectioned brain tissue (Figure 3.10F), which has not yet been confirmed with *ptch2* mRNA expression. The nuclear-GFP line does not accurately report *ptch2* mRNA expressed in the GC along the ventral RV (Figure 3.9R) or in diffuse cells in the hindbrain (data not shown).

D. Discussion

i. Overview of Hedgehog responsive regions in the adult zebrafish brain

Using both tissue sections and whole-brain imaging with FLSM we identified fourteen Hh responsive regions in the adult brain. From these regions, nine were identified as adult brain proliferative zones, seven of which were found along ventricular regions in the brain including the dorsal telencephalon (D), ventral telencephalon (V), hypothalamic (or diencephalic) ventricular region (DIV), periventricular gray zone (PGZ) of the optic tectum (TeO), midbrain-hindbrain border, cerebellum (Val), and the rhombencephalic ventricular zone (RV), as well as in two non-ventricular zones, the border between the olfactory bulbs (OBs) and telencephalon (Tel) and the torus longitudinalis (TL). The remaining five Hh responsive regions: the olfactory bulbs (OBs), dorsal entopenduncular nucleus (End), preglomerular nucleus (PGm), and disperse midbrain and hindbrain nuclei, were not identified proliferative zones in the adult brain. The nuclear-GFP line reported a subset of cell nuclei in six Hh responsive adult proliferative zones

(Figure 3.11B) and the nuclear-mCherry line also reported nuclei in six of the Hh responsive adult proliferative zones (Figure 3.11C). When used together both lines report transgene expression in eight of the nine Hh responsive adult proliferative zones, besides the TL (Figure 3.11). Table 2 describes the Hh responsive regions in the adult brain, as shown with *ptch2* mRNA expression from the *in situ*, whether the Hh responsive region is an adult proliferative zone, and whether the nuclear fluorescent protein expressing lines accurately report the Hh response in the brain region.

While neither line accurately reports *ptch2* mRNA expression throughout the brain, the lines are still useful for describing Hh responsive cells in regions where they do report *ptch2* mRNA expression accurately. In these region, nuclear-GFP and nuclear-mCherry may be used to quantify cells, as well as double labeling of cells with antibodies to determine cell type. Overall, *ptch2* mRNA expression most accurately displayed Hh responsive regions within the adult zebrafish brain.

ii. Potential roles for Hedgehog Signaling in the Adult Zebrafish Brain

a. Hh signaling may participate in a rostral migratory stream

The rostral migratory stream (RMS) is a well-studied pathway in the brain of adult mammals. In mammals, neuronal precursors generated in the subventricular zone (SVZ) of the lateral ventricle migrate to the olfactory bulbs (OBs) and differentiate into OB interneurons (Lois and Alvarez-Buylla, 1994). The SVZ is one of the few known proliferative zones in the adult mammalian brain, which indicates that the RMS is an important route for generating and transporting new cells in the brain. Interestingly, a similar RMS has been identified in the adult zebrafish brain (Kishimoto et al., 2011). Unlike adult mammals, the adult zebrafish brain has

many neurogenic zones located throughout the brain (Grandel et al., 2006). The telencephalic ventricular (TelV) zone is a particularly active neurogenic niche in the adult brain. In the ventral region of the TelV, neuronal precursors are generated and migrate anteriorly toward the medial side of the OBs. The neuronal precursors then migrate into the internal (ICL) and external (ECL) cellular layers of the OBs and differentiate into OB interneurons (Kishimoto et al., 2011).

Hh responsive cell nuclei are located along the ventral region of the TelV, at the junction between the Tel and OBs, as well as within the ICL and ECL of the OBs. Hh responsive nuclei within these regions indicate that Hh may play a role in the generation of the neuronal precursors in the ventral TelV and in their migration along the RMS towards the OBs. Hh responsive cell nuclei within the ICL and ECL of the OBs may indicate that these cells continue to respond to Hh as they migrate along the RMS to the OBs and may even play a role in their differentiation into OB interneurons.

b. Hh signaling in proliferative ventricular radial glia throughout the brain

Hh responsive cell nuclei are found along ventricular zones within the telencephalon, diencephalon, optic tectum, and rhombencephalon. These ventricular regions are known proliferative zones in adult zebrafish brain (Grandel et al., 2006). Hh responsive cells found in these proliferative ventricular regions may play a direct role in cell proliferation, differentiation, and migration. While it is known that ventricular regions have increased neurogenic ability, the role of Hh in these regions is largely unknown. In a subset of cells within these proliferative ventricular regions, Hh responsive cell nuclei overlapped with both PCNA and GFAP positive cells. This indicates Hh may play an important role in the proliferative potential of radial glia along the ventricular regions of the adult brain.

Progenitor cell regions within the telencephalon are the most studied in the adult zebrafish brain. The progenitor cells are clustered along the dorsal and ventral telencephalic ventricle. The dorsal domain is associated with slow cycling Type II neural progenitor cells and the ventral region is associated with transit amplifying Type III cells (Kizil et al, 2012). Hh responsive cell nuclei are observed mainly along the ventral TelV and to less of an extent along the dorsal TelV at the border of the telencephalon and olfactory bulbs. Neurons produced in ventral telencephalon progenitor cell niches migrate into the olfactory bulbs (Grandel et al, 2006), which may explain the increased neurogenic activity within the junction between these two regions. The TelV is homologous to the SVZ in mammals, which produces neurons that migrate to the olfactory bulbs via the RMS (Zhao et al, 2008).

The most active Hh responsive region of the adult zebrafish brain is located along the diencephalic ventricle (DIV). The DIV is a proliferative zone in the adult (Grandel et al., 2006) and is particularly active in Hh responsive cells, which may play a role in the neurogenic activity of this region. Based on PCNA overlap with Hh responsive cell nuclei along the DIV, it is thought that Hh may be acting on Type II slow cycling neural stem cells or Type III transit amplifying glioblasts. Hh responsive cells are found in dense clusters surrounding the medial, lateral, and posterior DIV using *Tg(GBS-ptch2:nlsEGFP)* and radial glial-like processes from the ventral region of the hypothalamus are observed extending into the pituitary using *Tg(GBS-ptch2:EGFP)*. The radial glial cells surrounding the DIV appear to be more actively proliferative along the medial DIV compared to both the lateral recess (LR) and posterior recess (PR) (Edelmann et al, 2013). This may indicate that Hh expression in the LR and PR may be active in Type II cells, whereas Hh expression in the medial DIV may be active in Type III cells.

Proliferative cells are found within the medial, lateral, and caudal region of the periventricular gray zone (PGZ) of the adult optic tectum (Schmidt et al, 2013). The PGZ is a region located ventral to the optic tectum and surrounds the tectal ventricle (TeV). Hh responsive cells are found dispersed throughout the area of the PGZ in the optic tectum of adult zebrafish. In the developing zebrafish tectum, eliminating Hh signaling shows a marked reduction in neural progenitor cell proliferation, whereas increasing Hh signaling has the opposite effect (Feijoo et al, 2011). The link between Hh and the proliferation of cells in the periventricular gray zone (PGZ) of the optic tectum may be retained from embryonic stages and continue to function to a lesser degree in adults. It is possible that cells generated in this region may have the ability to migrate into the tectum and replace older cells to maintain the functioning of the optic tectum. Hh responsive cells of the PGZ are thought to belong to a population of radial glial cells that are located in the ventral optic tectum facing the tectal ventricle (Kizil et al, 2012), however Hh responsive cells are seen in all regions of the PGZ and are not limited to the ventricular region. Hh responsive cells are found throughout layers 1-3 of the PGZ of the optic tectum from anterior-to-posterior. Layer 3 of the PGZ represents Type III Hh responsive radial glia reaching out to the TeV, while layers 1 and 2 represent Type II Hh non-radial glial Hh responsive cell types (Ito et al., 2010).

Hh responsive cell nuclei are found surrounding the rhombencephalic ventricle (RV), another known proliferative region in the adult zebrafish brain (Grandel et al., 2006). Hh is likely regulating the neurogenic ability of cells along the RV, which may serve a function in spinal cord regeneration observed in adult zebrafish (Reimer et al., 2009).

c. Hh signaling in endocrine precursors in the neurohypophysis

The pituitary gland, located ventral to the hypothalamus, is a non-proliferative zone within the adult zebrafish brain that actively responds to Hh signaling. Hh responsive cell nuclei and glial cell processes are seen within the pituitary and extending into the pituitary from the ventral hypothalamus indicating that Hh signaling may be associated with pituitary function. Hh may play a role in regulating endocrine function in the posterior pituitary, or neurohypophysis, by acting on pituicytes or tanycytes. While the exact role of Hh in the pituitary is unknown, the presence of Hh responsive post-mitotic cells in this region may indicate the importance of Hh in adult pituitary function.

iii. Overview of tissue preparation techniques

a. Transparent brains produces similar expression patterns observed in sectioned tissue

Using a protocol similar to CLARITY (adapted from Tomer et al., 2014), we prepared and imaged intact, transparent, adult zebrafish brains. The fixed and lipid cleared brain tissue enabled full brain imaging using fluorescent light sheet microscopy (FLSM). Using this procedure, we eliminated the need for frozen, thin sectioning of adult brain tissue to observe expression patterns. This procedure enabled both fast and efficient preparation and imaging of adult brain tissue when compared to other methods.

To prove the method of brain fixation and imaging was effective, we compared frozen sections of adult brain tissue imaged using confocal microscopy to z-stack images of transparent adult brain tissue using FLSM of the same fluorescent reporter line. We found that the expression patterns in transparent brain tissue were comparable to expression patterns observed in frozen tissue. Transparent brains produced similar GFP and mCherry expression intensity and generated tissue with persevered structure and histological features when prepared correctly. A

loss of fluorescent protein intensity or a complete loss of fluorescence was observed in brain tissue prepared with expired reagent. However, with the proper maintenance of reagents, these issues can be avoided. Therefore, we determined transparent adult brain tissue imaged using FLSM can produce both robust and accurate expression patterns and would be a useful technique for representing Hh signaling in the adult brain. As discussed in Chapter 2, we observed a loss of fluorescence in brains during tissue preparation. While the relatively low rate of brains with preserved fluorescence (~10%) did not prevent the analysis of the Hh reporters in this study, further optimization of the tissue preparation pipeline is needed before high-throughput imaging can be achieved.

b. Autofluorescence in the Hedgehog reporter lines

We observed GFP and mCherry expression within blood vessels of sectioned brain tissue prior to antibody labeling. To show that this expression was autofluorescence and not real expression, we compared transverse sections before and after antibody labeling. By labeling with anti-GFP and anti-mCherry antibodies, we found similar fluorescence in the blood vessels, but brighter Hh responsive cells. Autofluorescence was observed in the blood vessels of both transgenic and non-transgenic fish.

In the OBs, autofluorescence in the blood vessels appeared to increase after antibody labeling, which may reveal real expression in the blood vessels. The observed fluorescence may be explained by the presence of autofluorescent red blood cells within the vasculature. However, the fluorescence may also be caused by actual transgene expression in the blood vessels. Expression may be real or the nuclear localized GFP may be misdirected, based on placement of the transgene, causing expression in the blood vessels. However, this seems unlikely based on the lack of amplification of fluorescence in the blood vessels after antibody labeling. Blood

vessel autofluorescence was mainly observed in the highly vascularized olfactory bulbs and telencephalon and was less of an issue in the midbrain and hindbrain.

iv. Accuracy and usefulness of the Hedgehog reporter lines

We found that the nuclear-mCherry and nuclear-GFP lines were generally accurate when used together in recapitulating *ptch2* mRNA expression and were therefore useful for reporting Hh responsive cells in the adult brain. These lines only report Hh responsive cell nuclei and therefore were not useful in determining cell morphology or identifying axonal and glial connections within the brain. However, these lines were useful for determining the location of the Hh responsive cell bodies.

Cytoplasmic-GFP and membrane-mCherry were not selected for the atlas, because neither recapitulated *ptch2* mRNA expression accurately. Cytoplasmic-GFP did not recapitulate *ptch2* mRNA expression in many of the Hh responsive regions. However, this line shows cellular morphology by expressing GFP in the cytoplasm of Hh responsive cells, which is useful for documenting connections within the brain. Bright GFP expressing cellular processes are found extending into the pituitary from the ventral hypothalamus with this line, which may indicate Hh responsive pituicytes or tannecytes in this region of the brain. The cell body of these cells in thought to reside in the hypothalamus and not within the pituitary, based on the lack of Hh responsive cell nuclei in the pituitary in the nuclear lines.

Membrane-mCherry expresses mCherry in Hh responsive regions of the brain, but the intensity and location of the expression is not useful for determining Hh responsive cells. While this line was designed to express mCherry along the membrane of Hh responsive cells to reveal cellular type and morphology, we found that the membrane localizing CAAX motif has difficulty sending and distributing mCherry along the membrane. Certain brain regions had punctate

mCherry expression, similar to the nuclear lines, while other regions had diffuse mCherry expression. This line has weak mCherry expression, even after antibody labeling, which makes it difficult to tell whether expression is real or background. Weak expression made verifying the expression of the transgene to the *ptch2* mRNA expression difficult, therefore making the line less useful in adults.

Based on *ptch2* mRNA expression it seems like the promoter we chose (~1.2kb *ptch2-GBS-GBS* regulatory element) does report all Hh responsive regions in the adult brain. The expression of *ptch2* mRNA was reported in Hh responsive cells recapitulated by transgene expression in the nuclear fluorescent protein expressing lines except for the medial preglomerular nuclei (PGm). There was also substantially less transgene expression in the Val, TL, and PGZ compared to ptch2 mRNA expression. It is possible that when the *ptch2* promoter region was designed for the transgenic lines, a large portion of its regulatory region was omitted. Sequences in this region may have been important for transcriptional regulation in these brain regions and the removal of the sequences may account for the lack of expression in the transgenic lines.

The variability in the lines can be attributed to many factors including where the transgene was inserted into the genome. In Hh responsive region not recapitulated by transgene expression, the transgene may have been inserted in a region where expression in a certain responsive brain area was repressed and therefore was not observed. This may be indicative of the variability observed among the lines, as the insertion sites are undoubtable different. The relative intensity of mCherry may also serve as an issue in lines utilizing it as a fluorescent reporter gene. As observed in *Tg(GBS-ptch2:nlsmCh)* expression is brighter in areas that seem to have a higher density of responsive nuclei. This can be observed when comparing the relative

expression in the ventral and dorsal telencephalic ventricle. In *Tg(GBS-ptch2:mCh-CAAX)* we were unable to discern cell morphology or projections within the brain. This issue may be attributed to mCherry being a low intensity fluorescent protein, as observed in areas of diffuse expression, or instead an issue with the CAAX motif distributing mCherry evenly along the membrane, as observed in areas of punctate expression.

Regardless of the causes, the variability observed between the lines is a serious consideration when using these lines to define Hh responsive regions and cell types within the brain. Since neither the cytoplasmic or membrane lines appear to accurately report Hh responsive cells in the adult when compared to *ptch2* expression, we are limited to an understanding of where only Hh responsive cell nuceli are located. By lacking lines that report the Hh response in cell membranes and the cytoplasm, we are unable to make connections in the brain with responsive cell types and are also very limited in our ability to observe cell morphology or to hypothesize cell type.

To improve our understanding of the Hh response in the adult brain thebest option may be to make new transgenic lines with a more complete promoter. BAC (bacterial artificial chromosome) recombination allows for the cloning of very large genomic fragments >100kb. This technique may be ideal for generating transgenic lines, as the insertion may be large enough to contain regulatory elements of the gene, enabling expression patterns to more accurately represent endogenous expression (Sharan et al., 2009). Since the *ptch2* promoter is only ~1.2kb in length, we may be excluding these regulatory elements, which may explain a lack of expression in brain regions with the transgenic lines that are known to be Hh responsive. Although BAC recombination has obvious benefits by creating a more complete promoter, there are a few limitations with the new technique. Since PCR amplified DNA is usually used in

recombineering, products may occasionally acquire mutations. However, these mutations are often identified with sequencing and are removed. Another limitation is that the sequence of the target gene must be known, which is less of an issue with widely used model organisms like zebrafish.

We may also chose to replace mCherry in future lines and instead select a brighter red fluorescent protein, such as dTomato. Creating lines that report the Hh response in both the cytoplasm and nucleus with both green and red fluorescent protein may be the most beneficial option, as we will gain information on location of the cell body with the nuclear line and cell morphology with the cytoplasmic line. The CAAX motif utilized in the membrane lines appears to have an issue with distributing the fluorescent protein evenly or completely along the membrane. It appears to either congregate together in one region and in others is not strong enough at the membrane to report useful information on cell morphology. The cytoplasmic line could altogether replace the need for a line that reports the Hh response in cell membranes. *Tg(GBS-ptch2:GFP)* expression in the pituitary shows strong and clear responsive cells, and may be likely to report strong and clear expression in other Hh responsive regions.

Transgenic Line/ Abbreviated Name	Sub-Cellular Labeling	Fluorescent intensity	Stages Expressed	Accuracy of Hh Reporting in Adults
Tg(GBS-ptch2:nlsmCh) (Nuclear-mCherry)	Nucleus	**	Embryos, Larvae, Adults	Mostly accurate
Tg(GBS-ptch2:nlsGFP) (Nuclear-GFP)	Nucleus	***	Embryos, Larvae, Adults	Mostly accurate
Tg(GBS-ptch2:mCh-CAAX) (Membrane-mCherry)	Membrane	***	Embryos, Larvae, Adults	Moderately accurate; transgene expression does not show cell morphology
Tg(GBS-ptch2:GFP-CAAX) (Membrane-GFP)	Membrane	*	Embryos, Larvae	N/A
Tg(GBS-ptch2:mCh) (Cytoplasmic-mCherry)	Cytoplasm	**	Embryos, Larvae	N/A
Tg(GBS-ptch2:GFP) (Cytoplasmic-GFP)	Cytoplasm	**	Embryos, Larvae, Adults	Not accurate; transgene expression only in ventral hypothalamus and pituitary

Table 3.1: Several transgenic zebrafish reporter lines were used to document the Hh response in embryos, larvae, and adults. Six transgenic lines express GFP or mCherry in the nucleus, membrane, and cytoplasm of Hh responsive cells. Relative fluorescent intensity in 4dpf larvae are indicated by asterisks (* = weak intensity, *** = strong intensity). All lines report the Hh response in embryos and larvae, while only four lines continue to express their transgene in adult brains. There is variable accuracy in reporting the Hh response in the brain in the four adult expressing lines.

Brain regions expressing *ptch2* mRNA	Proliferative zone?	Accurate transgene expression in *Tg(GBS-ptch2:nlsmCh)*	Accurate transgene expression in *Tg(GBS-ptch2:nlsGFP)*
Olfactory bulbs (OBs) (ICL, ECL, GL)	No	Yes	No
OB and telencephalon (Tel) border	Yes	Yes, but in a very small subset of cells	Yes, but in a very small subset of cells
Dorsal Tel	Yes	Yes	Yes
End	No	Yes	No
Ventral Tel	Yes	Yes	Yes
PGZ of optic tectum (TeO)	Yes	No	Yes
Disperse midbrain cells	No	Yes	Yes
Region of DIV (hypothalamic ventricular region)	Yes	Yes, weak transgene expression in a small subset of cells	Yes, misexpression observed surrounding MFB
PGm	No	No	No
Midbrain and Hindbrain border	Yes	Yes	No
Cerebellum (Val)	Yes	No	Yes, very few cells
TL	Yes	No	No
RV (GC)	Yes	Yes	No
Disperse hindbrain cells (MLF, CC, LCa, and CCe)	No	Yes	No

Table 3.2: Nuclear fluorescent protein expressing Hh reporter lines can be used to show Hh responsive cells in a subset of proliferative zone in the adult zebrafish brain. The above chart describes adult brain regions that express *ptch2* mRNA, whether the regions are proliferative zones in the adult brain, and whether the nuclear-mCherry and nuclear-GFP lines accurately report Hh responsive cell nuclei in these regions.

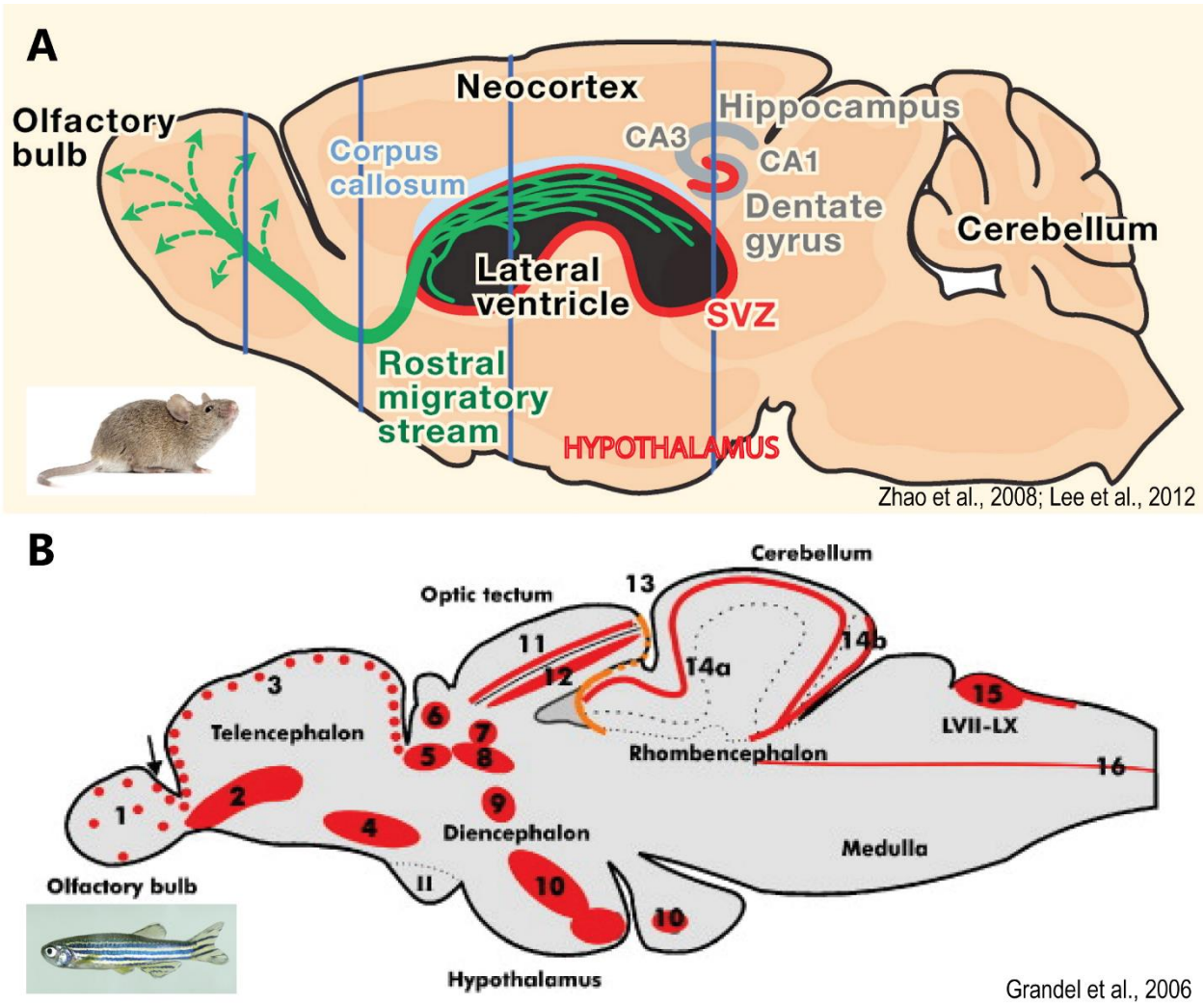

Figure 3.1: Proliferative zones in the adult mammalian and teleost brain. A) A schematic sagittal view of an adult mouse brain with 3 of the 8 known proliferative zones shown in red: SVZ of the forebrain lateral ventricle, SGZ of the dentate gyrus in the hippocampus, and the hypothalamus (Zhao et al., 2008; Lee et al., 2012). B) A schematic sagittal view of the adult zebrafish brain with 16 known proliferative zones shown in red: (1) border between the olfactory bulbs and dorsal telencephalon, (2) ventral telencephalon, (3) dorsal telencephalon, (4) preoptic region, (5) ventral thalamus, (6) habenular nuclei, (7) pretectal region, (8) dorsal thalamus, (9) posterior tuberculum, (10) hypothalamic ventricular region, (11) optic tectum, (12) torus longitudinalis, (13) border between the optic tectum and cerebellum, (14) (a) molecular and (b) granular layers of the cerebellum, (15) facial (LVII) and vagal (LX) lobes, and (16) rhombencephalic ventricular zone (Grandel et al., 2006).

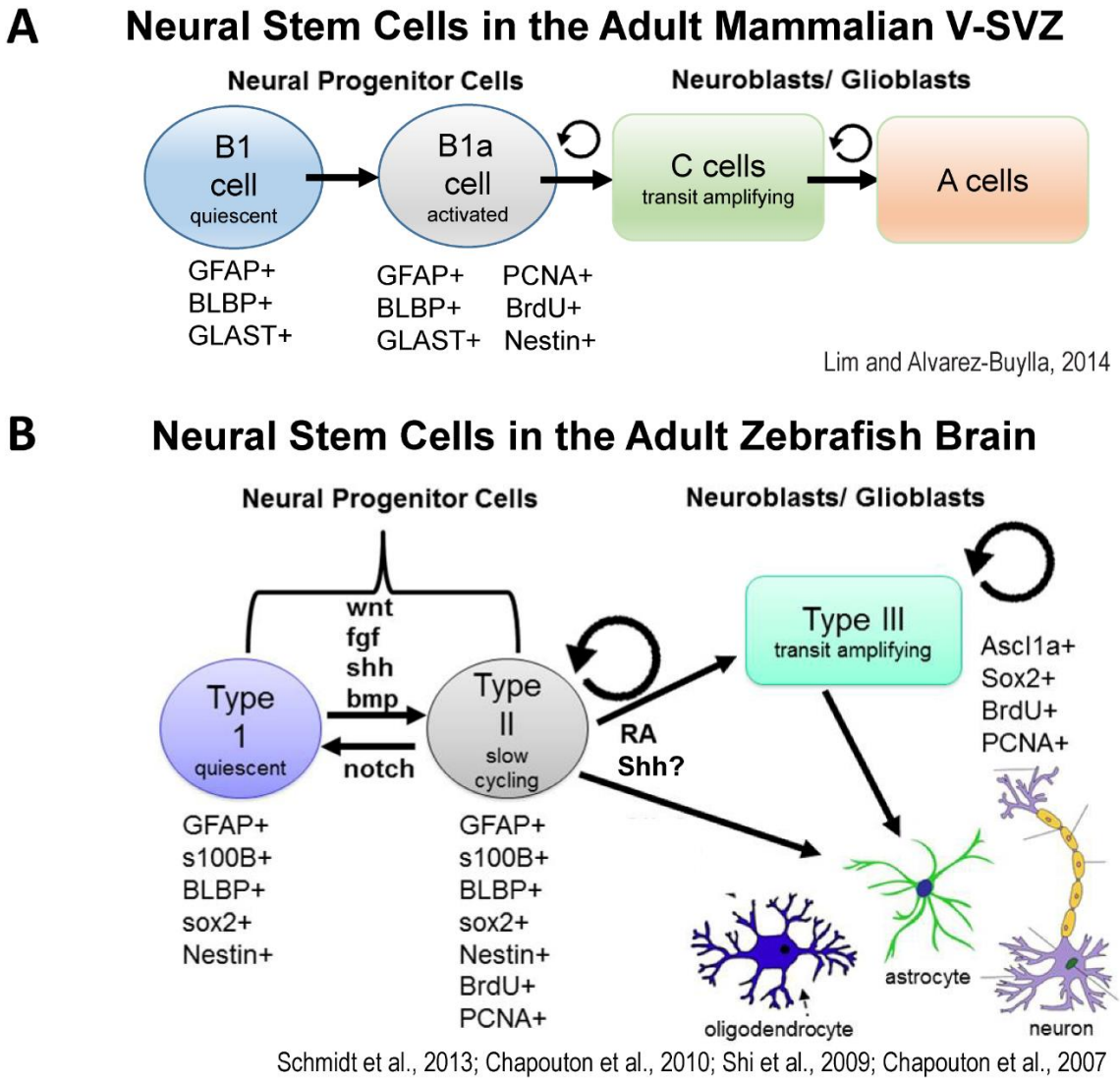

Figure 3.2: Neural stem cells in the adult mammalian V-SVZ and adult zebrafish brain. A) Quiescent B1 become activated B1 cells, which then divide to become transit amplifying C cells. C cells divide symmetrically to generate A cells, which are migratory neuroblasts that travel along the RMS to the olfactory bulbs (reviewed in Lim and Alvarez-Buylla, 2014). B) Once activated by a signal, Type I quiescent NSCs become slow cycling Type II NSCs that divide into differentiated neuronal and glial cell types or into Type III transit amplifying neuroblasts or glioblasts (reviewed in Schmidt et al, 2013; Chapouton et al, 2010; Shi et al, 2009; Chapouton et al, 2007).

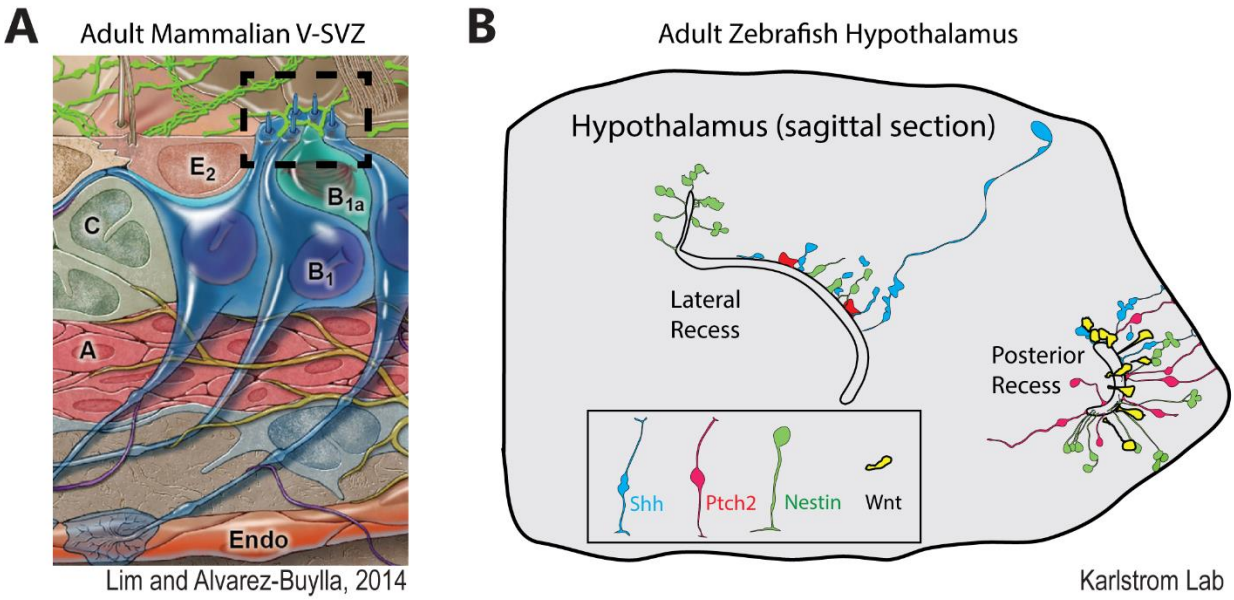

Figure 3.3: Hedgehog (Hh) signaling regulates neural stem cells (NSCs) along ventricular regions in the adult mammalian and zebrafish brain. A) In the adult mammalian V-SVZ, NSCs known as B1 cells, have a single primary cilium that faces the ventricular lumen (black dotted line box), providing a direct route for Shh to regulate their proliferative potential (C=C cells, A=A cells, E2=ependymal cells, B1= B1 cells, B1a=B1a cells, Endo=endothelial cells of blood vessel) (reviewed in Lim and Alvarez-Buylla, 2014). B) In the adult zebrafish hypothalamus, Shh producing cells (blue), Ptch2/Hh responsive cells (red), Nestin+ neural progenitor cells (green), and Wnt responsive cells (yellow) are found lining the lateral and posterior recess of the diencephalic ventricle (unpublished data from the Karlstrom lab).

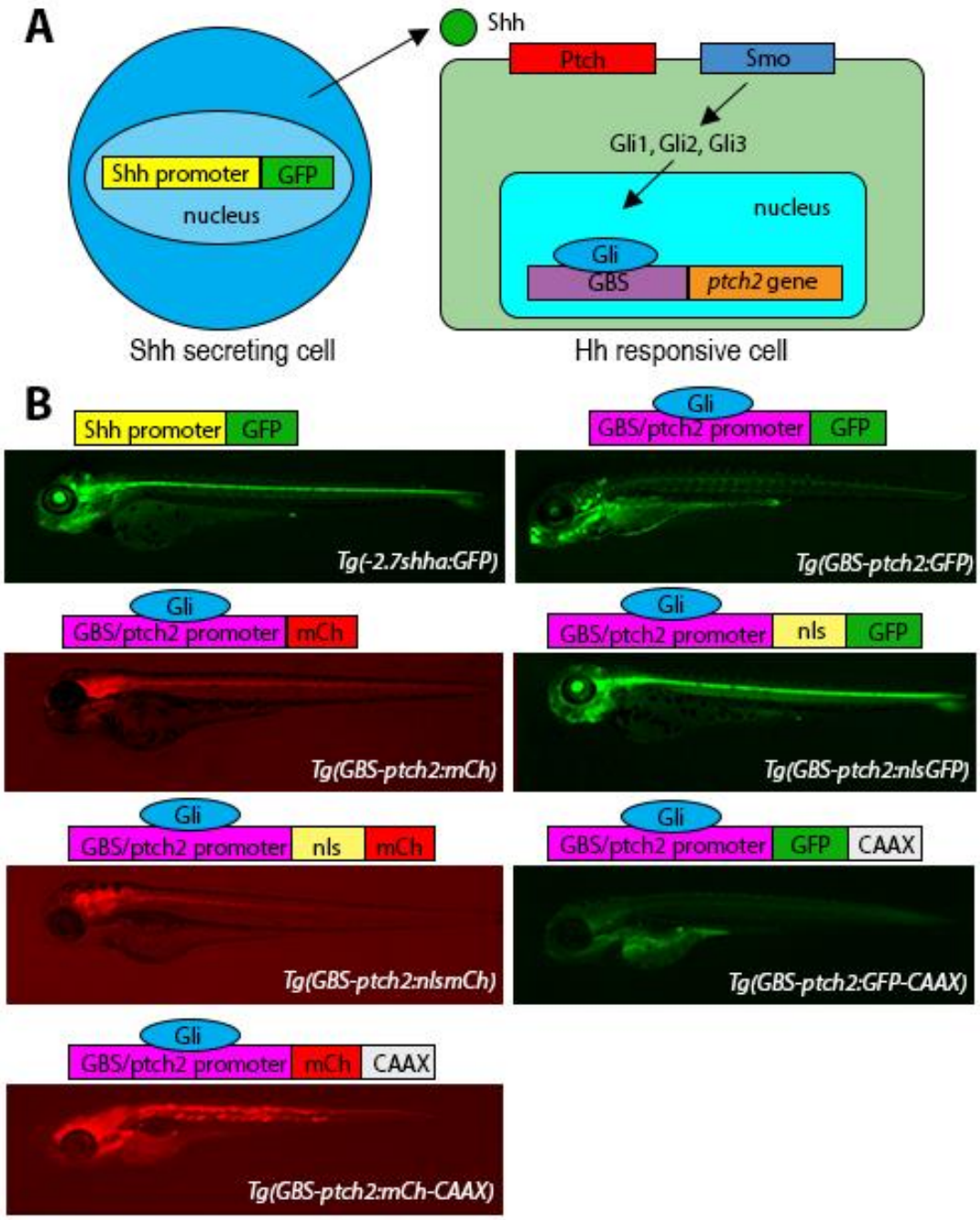

Figure 3.4: Fluorescent transgenic lines report cells producing and responding to Hh signaling in 4dpf larval zebrafish. A) Schematic of the Shh signaling pathway. B) The transgenic line *Tg(-2.7shha:GFP)* documents cells that produce the Shh signaling protein (Neumann and Nuesslein-Volhard, 2000). Six transgenic Hh reporter lines express GFP or mCherry in the nucleus, membrane, and cytoplasm of Hh responsive cells (Shen et al., 2013).

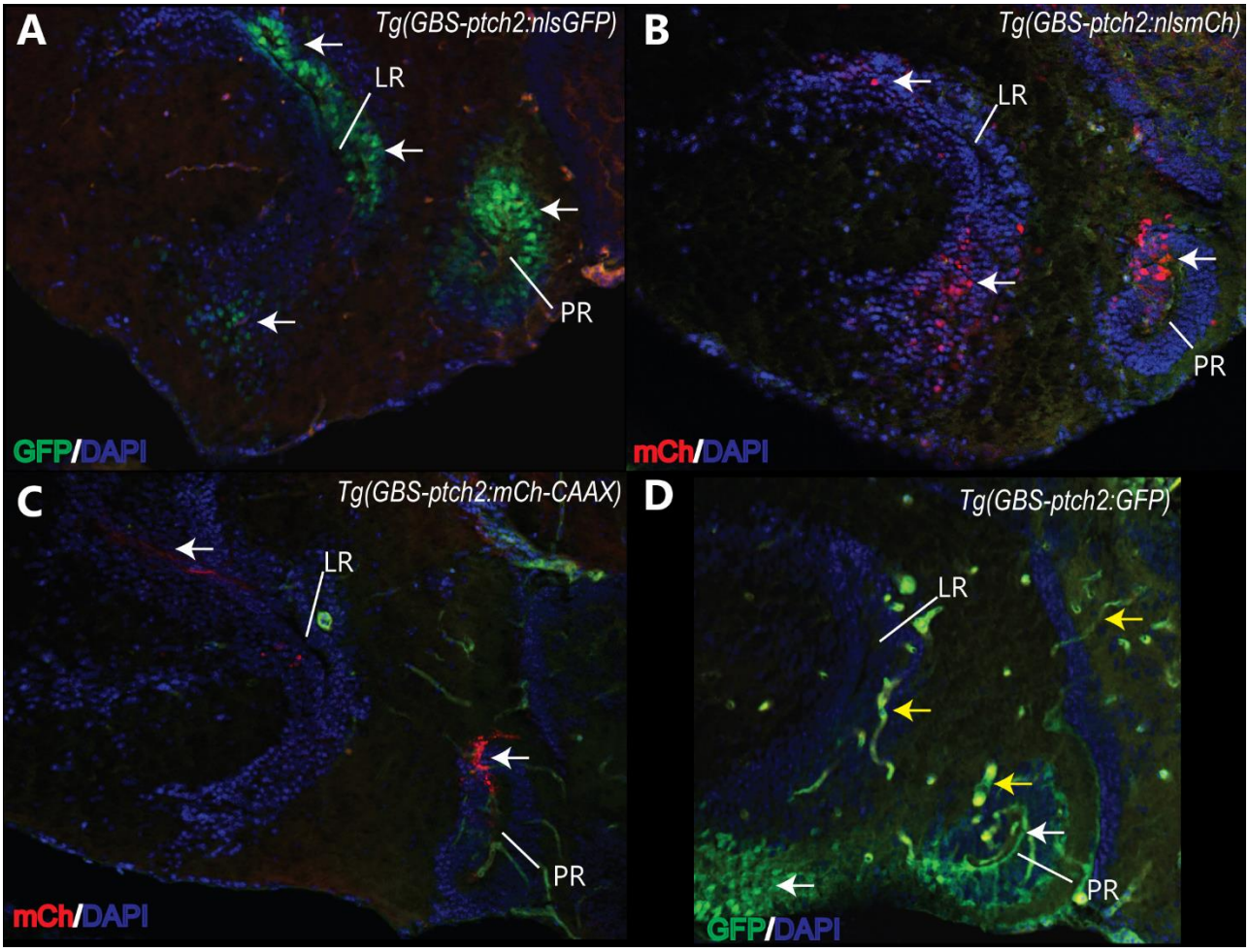

Figure 3.5: Variable expression patterns are observed along the lateral and posterior recess of the diencephalic ventricle in the ventral hypothalamus of 1 month old zebrafish from four Hedgehog reporter lines. Panels A-D are sagittal transverse sections in comparable regions of the diencephalic ventricle (DIV) that display both the lateral (LR) and posterior (PR) recesses. Hedgehog (Hh) responsive cells (either green or red) are found in these regions of the DIV. White arrows indicate transgene expression from the lines. Cell nuclei were stained with DAPI are seen in blue. A) Nuclear-GFP has clear and bright expression of Hh responsive cell nuclei (green) along the dorsal and ventral regions of the LR and along the dorsal region of the PR. B) Nuclear-mCherry has weak expression of Hh responsive cell nuclei (red) along the dorsal and ventral regions of the LR, as well as the dorsal region of the PR. Although weak, nuclei are still visible in these regions of the DIV. C) Membrane-mCherry has a diffuse Hh response (red) along the dorsal region of the LR and punctate expression along the dorsal region of the PR. D) Cytoplasmic-GFP reports Hh responsive cells (green) along the entire PR, including a few cells visible in the ventral region of the PR, as well as cells along the ventral region of the hypothalamus below the lateral recess. Yellow arrows indicate strongly autofluorescent blood vessels in this region that do not represent real transgene expression.

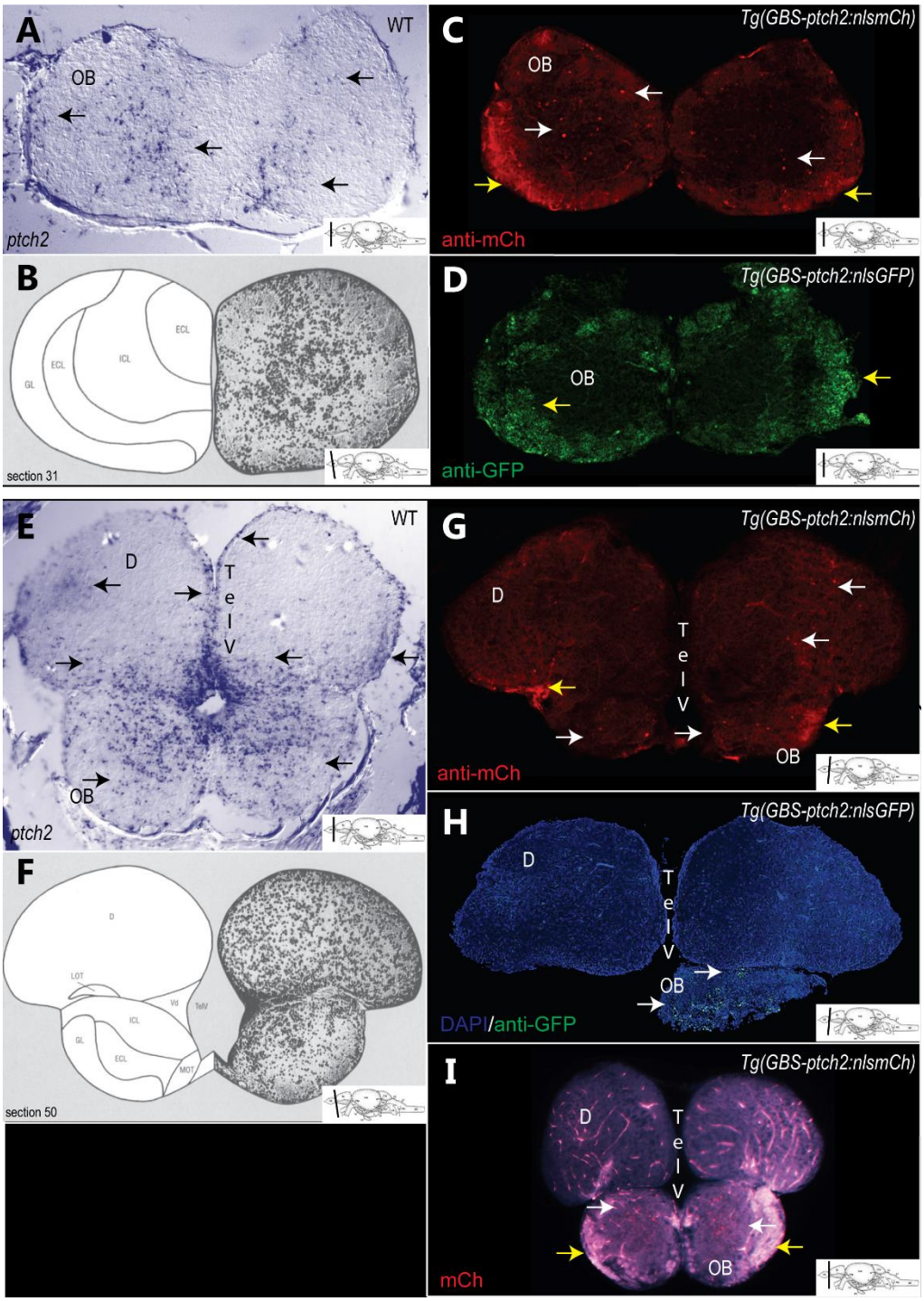

Figure 3.6: Hh responsive cells in the olfactory bulbs and at the olfactory bulb and dorsal telencephalon border. A) Black arrows indicate *ptch2* mRNA expression in the OBs. B) Schematic transverse section of the OBs at a location similar to the sections in panels A, C-D (Wullimann et al., 1996; section 31; ECL external cellular layer of olfactory bulb including mitral cells, GL: glomerular layer of olfactory bulb, ICL: internal cellular layer of olfactory bulb). C) Nuclear-mCherry shows the Hh response in discreet nuclei (red) within the OBs (white arrows). Autofluorescence in peripheral layers in the GL are indicated by yellow arrows. D) Nuclear-GFP shows no Hh responsive cell nuclei in the OBs. Autofluorescence in the GL is

indicated with yellow arrows. E) Black arrows indicate *ptch2* mRNA expression along the OB and D border, TelV, and in discreet nuclei within the D and OBs. F) Schematic transverse section of the border between the OB and D in a similar location to the sections in panels E, G-I (Wullimann et al., 1996; section 50; D: dorsal telencephalic area, ECL: external cellular layer of olfactory bulb including mitral cells, GL: glomerular layer of olfactory bulb, ICL: internal cellular layer of olfactory bulb, TelV: telencephalic ventricle, V: ventral telencephalic area, Vd: dorsal nucleus of V). G) Sectioned brain tissue from the nuclear-mCherry line shows Hh responsive cell nuclei (red) within the OBs (white arrows) and autofluorescence in the GL and ventro-lateral D (yellow arrows). H) Section brain tissue from the nuclear-GFP line shows Hh responsive nuclei (green) within the OBs (white arrows). I) Transparent whole adult brain from the nuclear-mCherry line imaged with FLSM shows Hh responsive cell nuclei in the OBs and at the OB and D border (white arrows), as well as autofluorescence in the GL (yellow arrows).

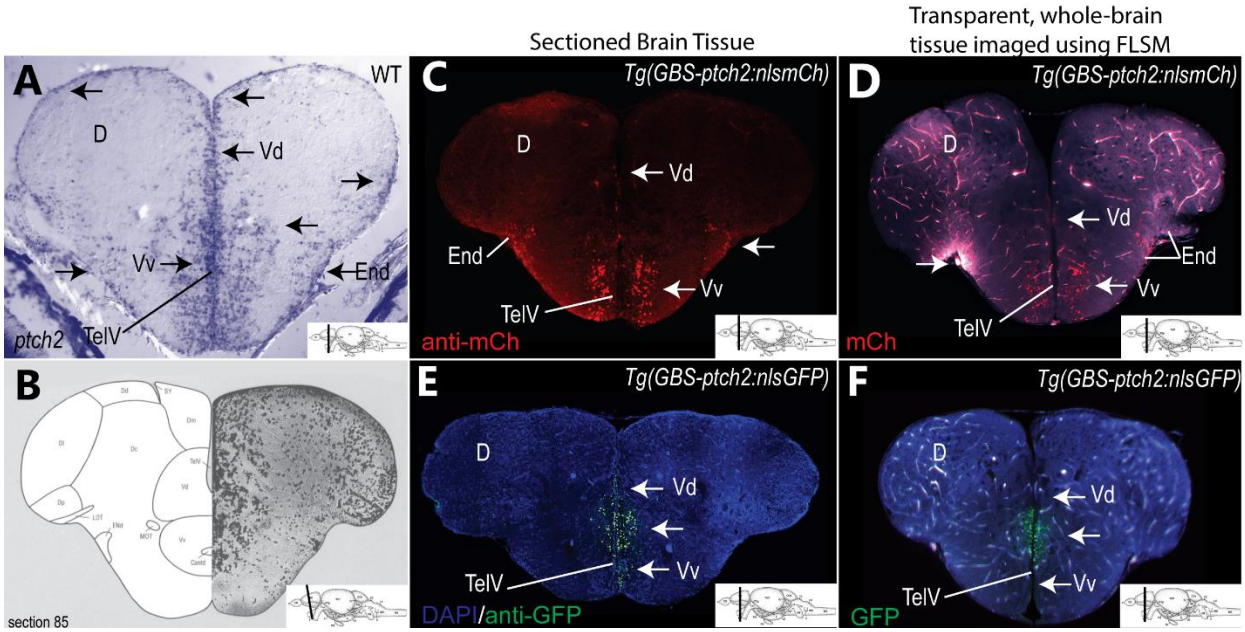

Figure 3.7: Hh responsive cells in the dorsal and ventral telencephalon. A) Black arrows indicate *ptch2* mRNA expression along the dorsal (Vd) and ventral (Vv) regions of the ventral telencephalic ventricle, along peripheral regions of the dorsal telencephalon (D), as well as within the dorsal entopenduncular nucleus (End). B) Schematic transverse section of the Tel at a location similar to the sections in panels A, C-F (Wullimann et al., 1996; section 85; TelV: telencephalic ventricle, Vd: dorsal region of ventral telencephalic ventricle, Vv: ventral region of ventral telencephalic ventricle, D: dorsal telencephalon, End: dorsal entopenduncular nucleus). C) Sectioned and D) transparent brain tissue from the nuclear-mCherry line shows Hh responsive nuclei (red) in a few cells along the TelV and End, with a large subset of cells in the Vv (white arrows). E) Sectioned and F) transparent brain tissue from the nuclear-GFP line express Hh responsive nuclei (green) in a few cells along the TelV with a large percentage of cells along the Vd (white arrows).

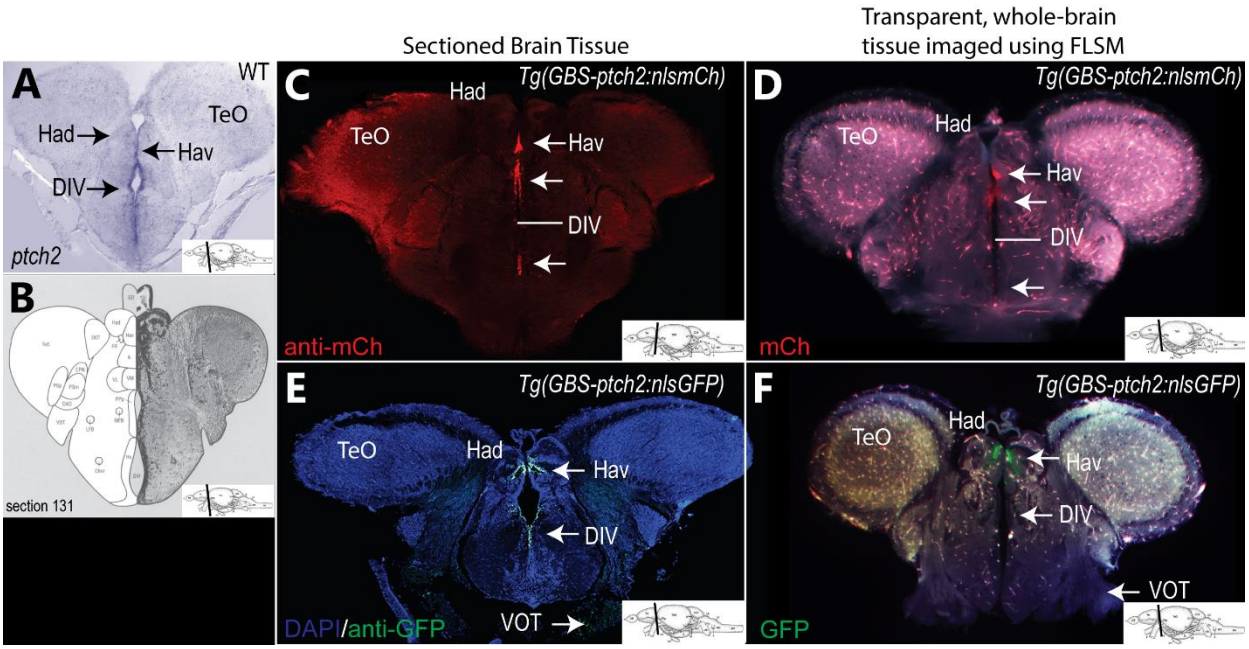

Figure 3.8: Hh responsive cells along the diencephalic ventricle. A) Black arrows indicate *ptch2* mRNA expression along the DIV in several nuclei including the A, VM, Ppp, Hv, as well as between the Hav. B) Schematic transverse section at a location similar to the sections in panels A, C-F (Wullimann et al., 1996; section 131; Had: dorsal habenular nuclei, Hav: ventral habenular nuclei, TeO: optic tectum, DIV: diencephalic ventricle, VOT: ventral optic tract). C) Sectioned and D) transparent brain tissue from the nuclear-mCherry line shows Hh responsive nuclei (red) between the Hav and along the DIV in the A, VM, and a few cells in the Hv (white arrows). E) Sectioned and F) transparent brain tissue from the nuclear-GFP line express Hh responsive nuclei (green) between the Had and Hav and in a few cells along the DIV (white arrows). Transgene expression is observed in the VOT in only sectioned tissue from this line.

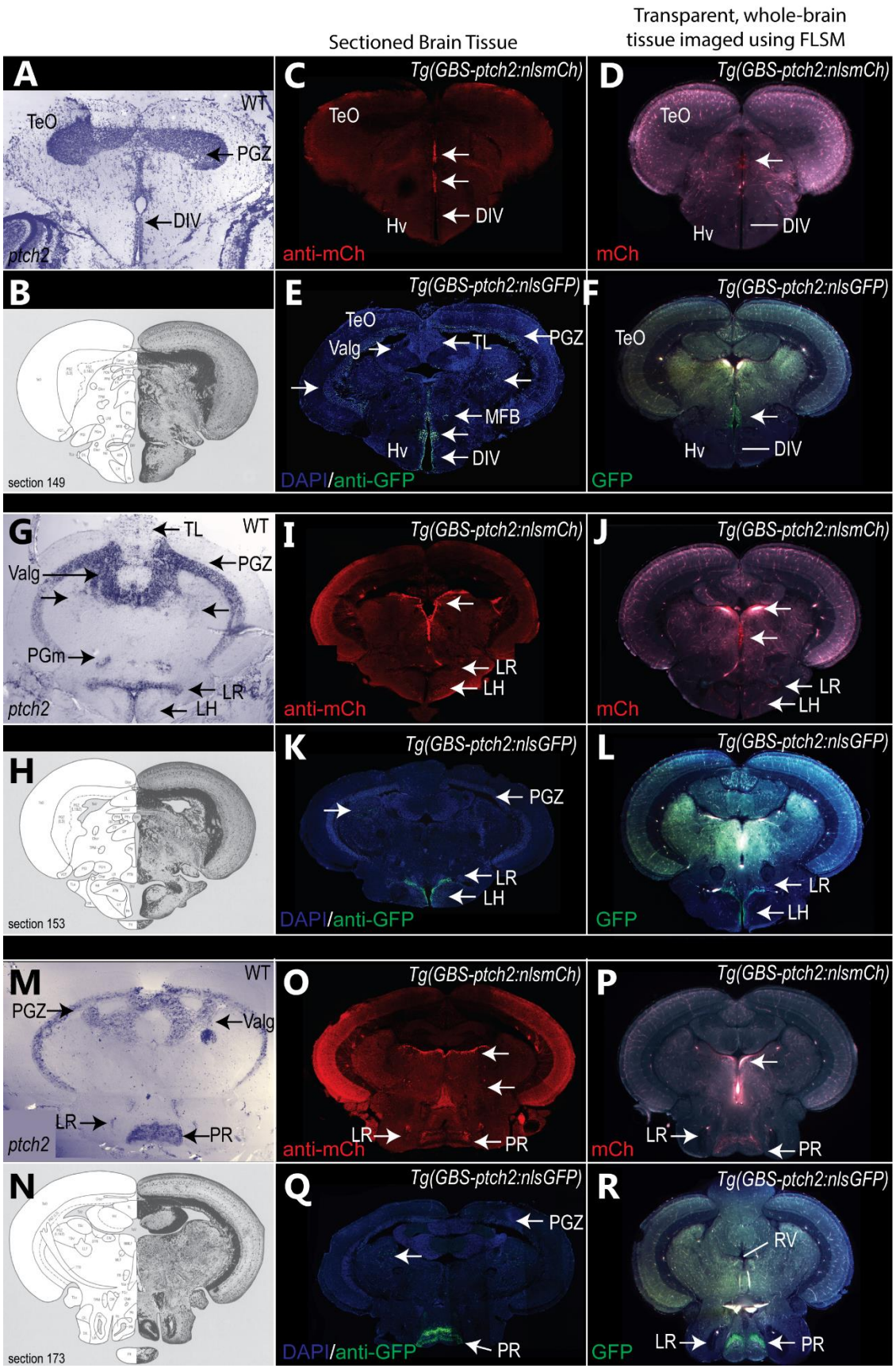
Sectioned Brain Tissue
Transparent, whole-brain tissue imaged using FLSM
A
WT
TeO
PGZ
DIV
ptch2
C
Tg(GBS-ptch2:nlsmCh)
TeO
Hv
DIV
anti-mCh
D
Tg(GBS-ptch2:nlsmCh)
TeO
Hv
DIV
mCh
B
section 149
E
Tg(GBS-ptch2:nlsGFP)
TeO
Valg
TL
PGZ
MFB
Hv
DIV
DAPI/anti-GFP
F
Tg(GBS-ptch2:nlsGFP)
TeO
Hv
DIV
GFP
G
WT
TL
PGZ
Valg
PGm
LR
LH
ptch2
I
Tg(GBS-ptch2:nlsmCh)
LR
LH
anti-mCh
J
Tg(GBS-ptch2:nlsmCh)
LR
LH
mCh
H
section 153
K
Tg(GBS-ptch2:nlsGFP)
PGZ
LR
LH
DAPI/anti-GFP
L
Tg(GBS-ptch2:nlsGFP)
LR
LH
GFP
M
WT
PGZ
Valg
LR
PR
ptch2
O
Tg(GBS-ptch2:nlsmCh)
LR
PR
anti-mCh
P
Tg(GBS-ptch2:nlsmCh)
LR
PR
mCh
N
section 173
Q
Tg(GBS-ptch2:nlsGFP)
PGZ
DAPI/anti-GFP
PR
R
Tg(GBS-ptch2:nlsGFP)
RV
LR
PR
GFP

Figure 3.9: Hh responsive cells in the optic tectum, in the diencephalic ventricular region, and in the cerebellum. A) Black arrows indicate *ptch2* mRNA expression in the PGZ of the TeO, along the DIV, and within discrete midbrain nuclei. B) Schematic transverse section of a location similar to the sections in panels A, C-F (Wullimann et al., 1996; section 149; TeO: optic tectum, PGZ: periventricular gray zone; DIV: diencephalic ventricle; Hv: ventral hypothalamus; Val: valvula cerebellum; TL: torus longitudinalis; MFB: medial forebrain bundle). C) Sectioned tissue from the nuclear-mCherry line shows Hh responsive cell nuclei (red) along the dorsal and dorso-medial regions of the DIV (white arrows). D) Optical section of cleared brain tissue from the nuclear-mCherry line shows Hh responsive nuclei (red) along the dorsal region of the DIV (white arrows). E) Sectioned tissue from the nuclear-GFP line shows Hh responsive cell nuclei (green) along the DIV, within the Hv, in the PGZ of the TeO, Val, TL, surrounding the MFB, and in discreet midbrain nuclei (white arrows). F) Optical section of cleared brain tissue from the nuclear-GFP line shows Hh responsive nuclei (green) along the dorsal region of the DIV (white arrows). G) Black arrows indicate *ptch2* mRNA expression in the PGZ of the TeO, along the DIV (in the LR and LH), Val, TL, PGm, and within discrete midbrain nuclei. H) Schematic transverse section of a location similar to the sections in panels G, I-L (Wullimann et al., 1996; section 153; PGZ: periventricular gray zone; LR: lateral recess of the diencephalic ventricle; LH: lateral hypothalamus; Val: valvula cerebellum; TL: torus longitudinalis; PGm: medial preglomerular nucleus). I) Sectioned tissue from the nuclear-mCherry line shows Hh responsive cell nuclei (red) along the ventral tectal ventricle and moving ventrally along the midline, as well as in a small subset of cells along the LR and LH (white arrows). J) Optical section of cleared brain tissue from the nuclear-mCherry line shows Hh responsive nuclei (red) along the ventral tectal ventricle and moving ventrally along the midline, as well as in a small subset of cells along the LR and LH (white arrows). K) Sectioned tissue from the nuclear-GFP line shows Hh responsive cell nuclei (green) along the LR and LH, in the PGZ of the TeO, and in discreet midbrain nuclei (white arrows). L) Optical section of cleared brain tissue from the nuclear-GFP line shows Hh responsive nuclei (green) along the LR and LH (white arrows). M) Black arrows indicate *ptch2* mRNA expression in the PGZ of the TeO, along the PR and LR of the DIV, and within discrete midbrain nuclei. N)) Schematic transverse section of a location similar to the sections in panels M, O-R (Wullimann et al., 1996; section 173; PGZ: periventricular gray zone; LR: lateral recess of the diencephalic ventricle; PR: posterior recess of the DIV; Val: valvula cerebellum). O) Sectioned tissue from the nuclear-mCherry line shows Hh responsive cell nuclei (red) along the ventral tectal ventricle and moving ventrally along the midline, as well as in a small subset of cells along the LR and PR of the DIV (white arrows). P) Optical section of cleared brain tissue from the nuclear-mCherry line shows Hh responsive nuclei (red) along the ventral tectal ventricle and moving ventrally along the midline, as well as in a small subset of cells along the LR and PR of the DIV (white arrows). Q) Sectioned tissue from the nuclear-GFP line shows Hh responsive cell nuclei (green) in the PGZ of the TeO, in discreet midbrain nuclei, and along the PR of the DIV (white arrows). R) Optical section of cleared brain tissue from the nuclear-GFP line shows Hh responsive nuclei (green) along the LR and PR of the DIV (white arrows).

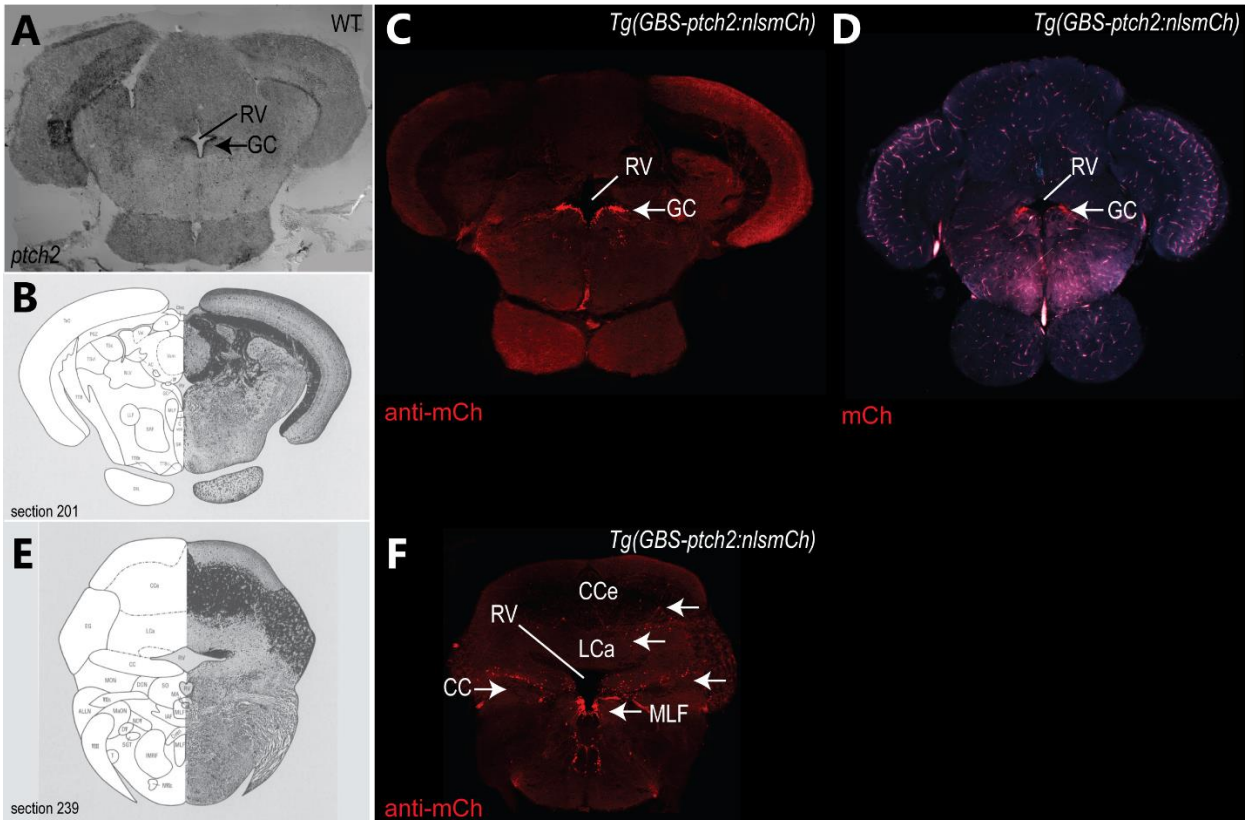

Figure 3.10: Hh responsive cells in the hindbrain and anterior spinal cord. A) Black arrows indicate *ptch2* mRNA expression along the ventral RV in the GC. B) Schematic transverse section at a location similar to the sections in panels A, C-D (Wullimann et al., 1996; section 201; RV: rhombencephalic ventricle, GC: griseum centrale). C) Sectioned and D) transparent brain tissue from the nuclear-mCherry line shows Hh responsive nuclei (red) along the ventral RV in the GC (white arrows). E) Schematic transverse section at a location similar to the sections in panels F (Wullimann et al., 1996; section 239; RV: rhombencephalic ventricle, CCe: cerebellar corpus, MLF: medial longitudinal fascicle, CC: cerebellar crest, LCa: caudal lobe of the cerebellum). E) Sectioned brain tissue from the nuclear-mCherry line shows Hh responsive nuclei (red) along the ventral RV, as well as in the CCe, LCa, CC, and MLF (white arrows).

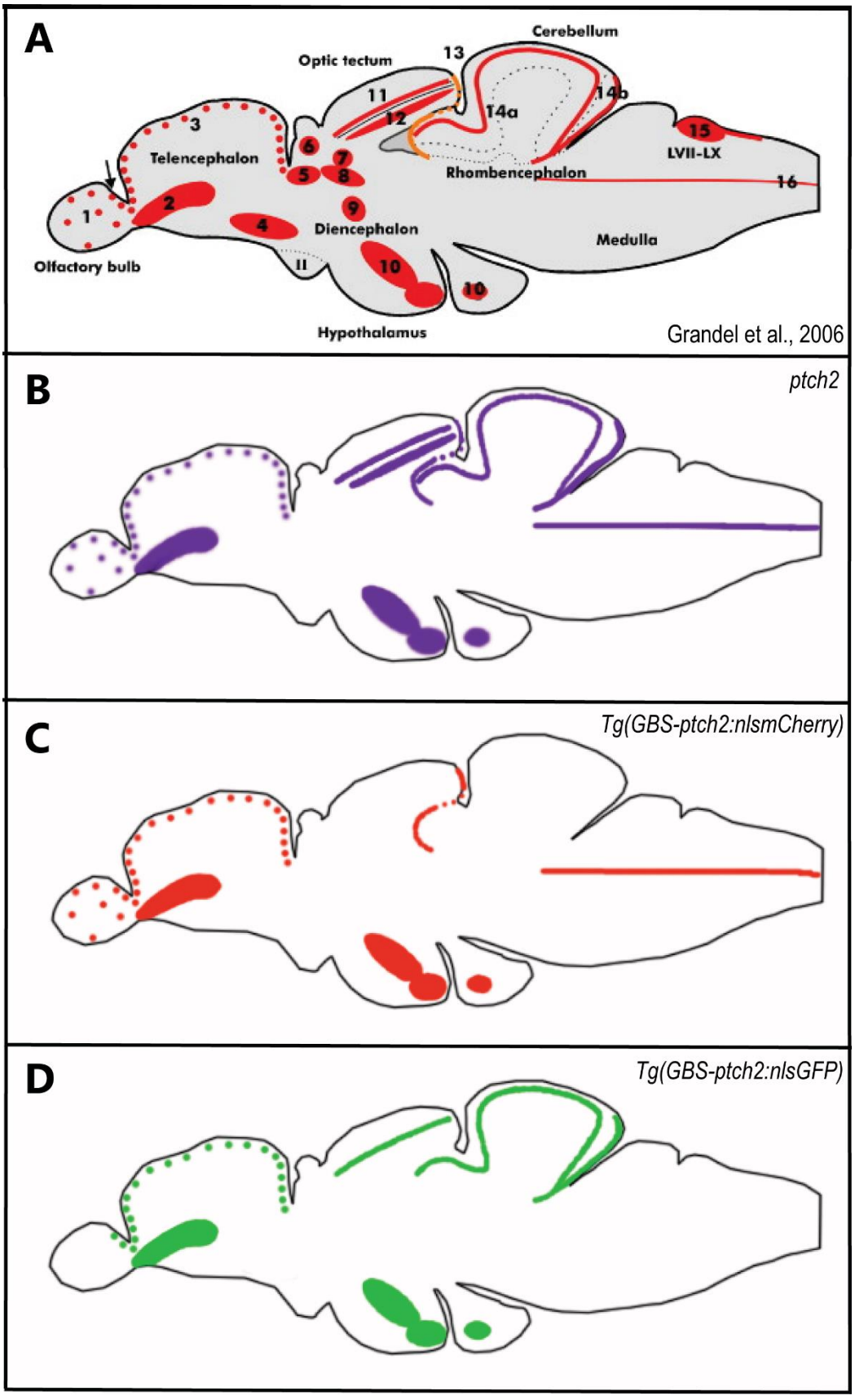
A
Cerebellum
Optic tectum
13
11
12
14a
14b
15
LVII-LX
3
Telencephalon
6
7
5
8
Rhombencephalon
16
1
2
9
4
Diencephalon
Medulla
Olfactory bulb
II
10
10
Hypothalamus
Grandel et al., 2006
B
ptch2
C
Tg(GBS-ptch2:nlsmCherry)
D
Tg(GBS-ptch2:nlsGFP)

Figure 3.11: Hh reporter lines express their transgene in the nuclei of a subset of Hh responsive proliferative zones. A) Sixteen proliferative zones remain active in the adult zebrafish brain (Grandel et al., 2006). B) Nine of the sixteen proliferative zones are responsive to the Hh signaling based on expression of the Hh responsive gene *ptch2* as seen with *in situ* hybridization (purple): olfactory bulbs (shown, but not a proliferative zone), (1) border between the olfactory bulbs and dorsal telencephalon, (2) ventral telencephalon, (3) dorsal telencephalon, (10) hypothalamic ventricular region, (11) optic tectum, (12) torus longitudinalis, (13) border between the optic tectum and cerebellum, (14) molecular and granular layers of the cerebellum, and the (16) rhombencephalic ventricular zone. C) The nuclear-mCherry Hh reporter line expresses its transgene in six of the nine Hh responsive adult proliferative zones (red): olfactory bulbs (shown, but not a proliferative zone), (1) border between the olfactory bulbs and dorsal telencephalon, (2) ventral telencephalon, (3) dorsal telencephalon, (10) hypothalamic ventricular region, (13) border between the optic tectum and cerebellum, and (16) rhombencephalic ventricular zone. D) The nuclear-GFP Hh reporter line also expresses its transgene in cells within six of the nine Hh responsive adult proliferative zones (green): (1) border between the olfactory bulbs and dorsal telencephalon, (2) ventral telencephalon, (3) dorsal telencephalon, (10) hypothalamic ventricular region, (11) optic tectum, and (14) molecular and granular layers of the cerebellum.

CHAPTER 4

CONCLUSION

The work presents the first gene expression atlases for an adult zebrafish brain, following the generation of similar atlases for the adult mouse and fly. Like other well established atlases, the ZABB will provide information ranging from annotated anatomical structures to the mapping of neural connections to gene expression and ISH hybridization data. However, this atlas will provide information that current atlases lack and will serve as a powerful tool for neuroscience research. So far we have developed tissue preparation and image processing pipelines that will be efficient for generating a high-throughput and open access community resource where other researchers can add their own data onto a reference brain image. The ZABB has both descriptive and functional applications, as well as potential clinical significance for understanding and treating neurodegenerative diseases and cancer. The functional aspect of the atlas will enable us to perform post-hoc analysis of neural activity, allowing us to identify neural circuits involved in simple and complex behaviors. This atlas may also be useful for identifying sex differences and studying the process of aging in the brain. Overall this atlas will be a useful resource for experiments focused on understanding brain function.

The Shh-signaling atlas presents a full description of the Hh response in the adult zebrafish brain with *ptch2* mRNA expression indicating Hh responsive cells. We have identified fourteen Hh responsive regions in the adult brain, nine of which are known proliferative zones. Using two transgenic lines that report Hh responsive cell nuclei, *Tg(GBS-ptch2:nlsGFP)* and *Tg(GBS-ptch2:nlsmCherry),* we were able to identify most of the Hh responsive regions. Between the two lines eight of the nine of the Hh responsive proliferative zones could be identified in the brain (excluding the torus longitudinalis), suggesting that when used together the

lines may be useful for understanding the role of Hh signaling in adult neurogenesis. Overall, we found that the lines were useful for describing Hh responsive brain regions that recapitulated *ptch2* mRNA expression as seen with ISH.

Using fluorescent transgenic lines to document Hh signaling in the brain has a variety of advantages over ISH. Transgenic lines allow us to identify cell type and morphology and may also enable us to identify the connections between Hh responsive cells in the brain. Unfortunately, both membrane and cytoplasmic Hh reporter lines failed to recapitulate *ptch2* mRNA expression, leaving the two nuclear reporter lines to document Hh responsive cells. The nuclear lines have limited our ability to observe cellular morphology and connections in the brain. It is possible that the generation of new transgenic reporter lines with a more complete *ptch2* promoter will solve the observed variation between lines and with ISH. However, the inconsistencies between the lines and ISH may reveal that *ptch2* is not an effective indicator of Hh signaling. Basal levels of *ptch2* may be expressed even when Hh is not present, which may explain the higher percentage of *ptch2* mRNA expressing cells with ISH when compared to transgene expression in the lines. Therefore, in the future other Hh target genes should be considered in the generation of the atlas.

By adding the nuclear Hh-reporter lines to the ZABB we have the ability to identify the relationship between Hh responsive cells and cells responding to other cell-cell signaling systems or cells of a specific type. We hope that this wok will improve our understanding of the cellular and molecular mechanisms behind adult neurogenesis, specifically the role of Hh in regulating neural progenitor cell populations in the adult brain. The knowledge gained and experiments executed using these atlases may be useful in identify new treatment options for a variety of neurodegenerative diseases and cancers.

REFERENCES

Adolf, B., Chapouton, P., Lam, C.S., Topp, S., Tannhauser, B., Strähle, U., Gotz, M., and Bally-Cuif, L. 2006. Conserved and acquired features of adult neurogenesis in the zebrafish telencephalon. *Dev. Biol.* 295(1), 278-293.

Altman, J. and Das, G. D. 1965. Autoradiographic and histological evidence of postnatal hippocampal neurogenesis in rats. *J Comp Neurol.* 124(3), 319-35.

Altman, J. and Das G. D. 1966. Autoradiographic and histological studies of postnatal neurogenesis. I. A longitudinal investigation of the kinetics, migration and transformation of cells incorporating tritiated thymidine in neonate rats, with special reference to postnatal neurogenesis in some brain regions. *J Comp Neurol.* 126(3), 337-89.

Altman J. 1969. Autoradiographic and histological studies of postnatal neurogenesis. IV. Cell proliferation and migration in the anterior forebrain, with special reference to persisting neurogenesis in the olfactory bulb. *J Comp Neurol.* 137(4), 433-57.

Araújo, G. L., Araújo, J. A., Schroeder, T., Tort, A. B. and Costa, M. R. 2014. Sonic hedgehog signaling regulates mode of cell division of early cerebral cortex progenitors and increases astrogliogenesis. *Front Cell Neurosci* 11, 77.

Arrenberg, A. B. and Driever, W. 2013. Integrating anatomy and function for zebrafish circuit analysis. *Front Neural Circuits* 7, 74.

Briscoe, J. and Therond, P. P. 2013. The mechanisms of Hedgehog signaling and its roles in development and disease. *Nat Rev Mol Cell Biol* 14, 416-29.

Chapouton, P., Jagasia, R., and Bally-Cuif, L. 2007. Adult neurogenesis in non-mammalian vertebrates. *BioEssays* 29, 745-757.

Chapouton, P., Skupien, P., Hesl, B., Coolen, M., Moore, J. C., Madelaine, R., Kremmer, E., Faus-Kessler, T., Blader, P., Lawson, N. D. and Bally-Cuif, L. 2010. Notch activity levels control the balance between quiescence and recruitment of adult neural stem cells. J. *Neurosci* 23, 7961-7974.

Chung, K. and Deisseroth, K. 2013. CLARITY for mapping the nervous system. *Nature Methods* 10, 508–513.

De Carlos J. A. and Borrell J. 2007. A historical reflection of the contributions of Cajal and Golgi to the foundations of neuroscience. *Brain Res Rev* 55(1), 8-16.

Edelmann, K., Glashauser, L., Sprungala, S., Hesl, B., Fritschle, M., Ninkovic, J., Godinho, L. and Chapouton, P. 2013. Increased radial glia quiescence, decreased reactivation upon injury and unaltered neuroblast behavior underlie decreased neurogenesis in the aging zebrafish telencephalon. *J Comp Neurol* 13, 3099-3115.

Feijoo, C.G., Oñate, M.G., Milla, L.A., and Palma, V.A. 2011. Sonic hedgehog (Shh)-Gli signaling controls neural progenitor cell division in the developing tectum in zebrafish. *Eur. J. Neurosci* 33(4), 589-598.

Ganz, J., Kaslin, J., Hochmann, S., Freudenreich, D., and Brand, M. 2010. Heterogeneity and Fgf dependence of adult neural progenitors in the zebrafish telencephalon. *Glia* 58(11), 1345-1363.

Grandel, H., Kaslin, J., Ganz, J., Wenzel, I. and Bond, M. (2006). Neural stem cells and neurogenesis in the adult zebrafish brain: Origin, proliferation dynamics, migration and cell fate. *Dev Bio* 295, 263-277.

Grant, G. 2006. How the 1906 Nobel Prize in Physiology or Medicine was shared between Golgi and Cajal. *Brain Res Rev* 55(2), 490-498.

Herculano-Houzel, S. 2012. The remarkable, yet not extraordinary, human brain as a scaled-up primate brain and its associated cost. *Proc Natl Acad Sci USA* 109, 10661-8 doi: 10.1073/pnas.1201895109.

Ingham, P.W. and McMahon, A.P. 2001. Hedgehog signaling in animal development: Paradigms and principles. *Genes & Dev.* 15, 3059–3087.

Ihrie, R. A., Shah, J. K., Harwell, C. C., Levine, J. H., Guinto, C. D., Lezameta M., Kriegstein, A. R., and Alvarez-Buylla, A. 2011. Persistent sonic hedgehog signaling in adult brain determines neural stem cell positional identity. *Neuron* 71, 250 –262.

Itoa, Y., Tanakaa, H., Okamotoa, H., and Ohshima, T. 2010. Characterization of neural stem cells and their progeny in the adult zebrafish optic tectum. *Dev Biol.* 342(1), 26-38.

Jones, A. R., Overly, C. C., and Sunkin, S M. 2009. The Allen Brain Atlas: 5 years and beyond. *Nature Reviews Neuroscience* 10, 821-828.

Kishimoto, N., Alfaro-Cervello, C., Shimizu, K., Asakawa, K., Urasaki, A., Nonaka, S., Kawakami, K., Garcia-Verdugo, J.M., and Sawamoto, K. 2011. Migration of neuronal precursors from the telencephalic ventricular zone into the olfactory bulb in adult zebrafish. *J Comp Neurol* 519(17), 3549-65.

Kizil, C., Kaslin, J., Kroehne, V. and Brand, M. 2012. Adult neurogenesis and brain regeneration in zebrafish. *Dev Neurobiol* 72, 429–461.

Klein, S., Staring, M., Murphy, K., Viergever, M. A., and Pluim, J. P. 2010. Elastix: a toolbox for intensity-based medical image registration. *IEEE Transactions on Medical Imaging* 29, 196-205.

Lam, E.Y., Chau, J.Y., Kalev-Zylinska, M.L., Fountaine, T.M., Mead, R.S., Hall, C.J., Crosier, P.S., Crosier, K.E., and Flores, M.V. 2009. Zebrafish runx1 promoter-EGFP transgenics mark discrete sites of definitive blood progenitors. *Blood* 113(6). 1241-1249.

Lee, D. A., Bedont, J. L., Pak, T., Wang, H., Song, J., Miranda-Angulo, A., Takiar, V., Charubhumi, V., Balordi, F., Takebayashi, H., Aja, S., Ford, E., Fishell, G., and Blackshaw, S. 2012. Tanycytes of the hypothalamic median eminence form a diet-responsive neurogenic niche. *Nat Neurosci.* 15, 700-702.

Lee, D. A. and Blackshaw, S. 2014. Feed your head: neurodevelopmental control of feeding and metabolism. *Annu. Rev. Physiol.* 76, 197–223.

Lehtinen, M. K., Zappaterra, M. W., Chen, X., Yang, Y., and Hill, A. 2011. The cerebrospinal fluid provides a proliferative niche for neural progenitor cells. *Neuron* 69, 893–905.

Lim, D. A. and Alvarez-Buylla, A. 2014. Adult neural stem cells stake their ground. *Trends Neurosci.* 37(10), 563-71.

Lois, C. and Alvarez-Buylla, A. 1994. Long-distance neuronal migration in the adult mammalian brain. *Science* 264(5162), 1145-8.

Marquart, G. D., Tabor, K. M., Brown, M., Strykowski, J. L., Varshney, G. K., LaFave, M. C., Mueller, T., Burgess, S. M., Higashijima, S., and Burgess, H. A. 2015. A 3D Searchable Database of Transgenic Zebrafish Gal4 and Cre Lines for Functional Neuroanatomy Studies. *Front Neural Circuits* 9, 78.

Martínez, C., Cornejo, V. H., Lois, P., Ellis, T., Solis, N. P., Wainwright, B. J., and Palma V. 2013. Proliferation of murine midbrain neural stem cells depends upon an endogenous sonic hedgehog (Shh) source. *PLoS One* 6, e65818.

März, M., Schmidt, R., Rastegar, S., and Strähle, U. 2010. Expression of the transcription factor Olig2 in proliferating cells in the adult zebrafish telencephalon. *Dev. Dyn.* 239(12), 3336-3349.

Menegas, W., Bergan, J. F., Ogawa, S., K., Isogai, Y., Venkataraju, K. U., Osten, P., Uchida, N., and Watabe-Uchida, M. 2015. Dopamine neurons projecting to the posterior striatum form an anatomically distinct subclass. *eLife* 4:e10032.

Milyaev, N., Osumi-Sutherland, D., Reeve, S., Burton, N., Baldock, R. A., and Armstrong, J. D. 2012. The Virtual Fly Brain browser and query interface. *Bioinformatics* 28, 411-415.

Ming, G. and Song, S. 2011. Adult Neurogenesis in the Mammalian Brain: Significant Answers and Significant Questions. *Neuron* 70, 687-702.

Neumann, C. J. and Nuesslein-Volhard, C. 2000. Patterning of the zebrafish retina by a wave of sonic hedgehog activity. *Science* 289(5487), 2137-9.

Parichy, D. M., Elizondo, M. R., Mills, M. G., Gordon, T. N., and Engeszer, R. E. 2009. Normal table of postembryonic zebrafish development: Staging by externally visible anatomy of the living fish. *Dev. Dyn.* 238(12), 2975-3015.

Petrova, R. and Joyner A. L. 2014. Roles for Hedgehog signaling in adult organ homeostasis and repair. *Development* 141, 3445-57.

Randlett, O., Wee, C. L., Naumann, E. A., Nnaemeka, O., Schoppik, D., Fitzgerald, J. E., Portugues, R., Lacoste, A. M. B., Riegler, C., Engert, F., and Schier, A. F. 2015. Whole-brain activity mapping onto a zebrafish brain atlas. *Nat Meth* 12, 1039-1046.

Ronneberger, O., Liu, K., Rath, M., Ruebeta, D., Mueller, T., Skibbe, H., Drayer, B., Schmidt, T., Filippi, A., Nitschke, R., Brox, T., Burkhardt, H., and Driever, W. 2012. ViBE-Z: a framework for 3D virtual colocalization analysis in zebrafish larval brains. *Nat Methods* 9, 735-742.

Reimer, M. M., Kuscha, V., Wyatt, C., Sörensen, I., Frank, R. E., Knüwer, M., Becker, T., and Becker, C. G. 2009. Sonic hedgehog is a polarized signal for motor neuron regeneration in adult zebrafish. *J. Neurosci.* 29, 15073–15082.

Schmidt, R., Strähle, U. and Scholpp, S. 2013. Neurogenesis in zebrafish – from embryo to adult. *Neural Development* 8(3).

Sharan, S. K., Thomason, L. C., Kuznetsov, S. G., and Court D., L. 2009. Recombineering: a homologous recombination-based method of genetic engineering. *Nat Protoc.* 4(2), 206-23.

Shen, M., Ozacar, A. T., Osgood, M., Boeras, C., Pink, J., Thomas, J., Kohtz, J., and Karlstrom, R. O. 2013. Heat-shock–mediated conditional regulation of hedgehog/gli signaling in zebrafish. *Dev. Dyn.* 242(5), 539-49.

Shi Y., Sun G., Zhao C., and Stewart R. 2009. Neural Stem Cell Self-renewal. *Crit Rev Oncol Hematol* 65, 43-53.

Sunkin, S. M., Ng, L., Lau, C., Dolbeare, T., Gilbert, T. L., Thompson, C. L., Hawrylycz, M., and Dang, C. 2013. Allen Brain Atlas: an integrated spatio-temporal portal for exploring the central nervous system. *Nucleic Acids Res*., D996–D1008.

Tomer, R., Ye, L., Hsueh, B., and Deisseroth, K. 2014. Advanced CLARITY for rapid and high-resolution imaging of intact tissues. *Nature Protocols* 9, 1682–1697.

White, J. G., Southgate, E., Thomson, J. N., Brenner, S. 1986. The structure of the nervous system of the nematode C. elegans. *Philos. Trans. R. Soc. Lond. B Biol. Sci.* 314, 1–340.

Wilt, B. A., Burns, L. D., Wei Ho, E. T., Ghosh, K. K., Mukamel, E. A., and Schnitzer, M. J. 2010. Advances in Light Microscopy for Neuroscience. *Annu Rev Neurosci* 32, 435.

Wong, S. Y. and Reiter, J. F. 2008. The primary cilium at the crossroads of mammalian hedgehog signaling. *Curr Top Dev Biol.* 85, 225-60.

Wullimann, M. F., Rupp, B. and Reichert H. 1996. Neuroanatomy of the Zebrafish Brain: A Topological Atlas. Boston: Birkhäuser.

Zhao C., Deng W., and Gage F. H. 2008. Mechanisms and Functional Implications of Adult Neurogenesis. *Cell* 132, 645-660.